Response to the reviewer 1 of the manuscript: "Comparison of different droplet measurement techniques in the Braunschweig Icing Wind Tunnel" by Inken Knop et al.

This manuscript describes an icing tunnel test facility that may be of interest to the atmospheric science community. The fundamental operation of this system is similar to existing icing tunnels, however, there is no comparison to icing tunnels that have been in existence for nearly 50 years. Of particular interest is the icing tunnel in Ottawa, Canada that is operated by the National Research Council. A description of the NRC icing tunnel can be found at https://nrc.canada.ca/en/research-development/nrc-facilities/altitude-icing-wind-tunnel- research-facility, and early papers describing experiments in the tunnel are by Strapp and Schemenauer (1982) and King et al. (1985). The NRC icing tunnel has unique advantages over the Braunschweig tunnel, specifically the NRC tunnel is capable of particle speeds up to 100 m s^{-1} and altitudes to 40,000 ft (12 km). The Braunschweig maximum particle speed of the Braunschweig tunnel is 40 m s^{-1} and it has not capacity to simulate altitude. This is unfortunate since research aircraft fly at various altitudes and all large aircraft fly at speeds that are at least twice the maximum speed that the Braunschweig tunnel can produce. The manuscript needs to discuss how the limitations of the Braunschweig tunnel influence their results.

Response: There are indeed many icing wind tunnels worldwide. The authors are well aware of the NRC facilities and have many excellent collaborations with the research teams in Canada. However, the goal of our paper is not to perform a tunnel-intercomparison exercise. Instead, we focus on the intercomparison of several droplet sizing techniques in one tunnel, the Braunschweig Icing Wind Tunnel.

The Braunschweig Icing Wind Tunnel has many applications, not only limited to aircraft icing. Also the presented measurement techniques are not only limited to applications in civil aviation. Therefore, the maximum speed of the tunnel and its sea level pressurization do not impede the validity of the results presented.

Nevertheless, we want to mention that numerous scaling methods based on similitude of geometry, droplet trajectories and the impingement heat transfer have been developed to scale the model and test conditions to simulate the conditions beyond the IWT abilities. A comprehensive description of the scaling methods can be found in Anderson (2004). Scaling one of the parameters requires changes in other parameters to maintain the similitude, often it is not possible to concurrently match all the similarity parameters, especially the pressure which in most of the tunnels cannot be controlled. The AIWT operated by NRC and CIRA icing wind tunnel have the ability to control the pressure to simulate the high altitude icing conditions. Anderson (2004) reports the factors that highly are highly sensitive to pressure have only a limited influence on the parameters that influence the icing the most. From the icing data available at AEDC Barlett (1988) states the influence of pressure on icing is insignificant, the joint NRC CIRA experiments to study the effect of pressure (Oleskiw et al. 1996) showed "relatively small changes in the forward-facing portion of the profiles".

We have modified the paper to include some of the above mentioned comments, and also mentioned the NRC facility in the introduction section.

Understanding discrepancies between drop concentrations and drop size distributions (PSDs) measured by various probes is of critical importance for cloud physics, albeit icing studies rely more on bulk quantities such as MVD and LWC. MVD and LWC are presented and discussed in great detail, but there is almost no quantitative discussion of drop concentrations and PSDs from the PDI, FCDP and Shadowgraphy instrumentation. The manuscript needs to include additional Figures that show correlations between reported drop concentrations and PSDs measured by PDI, FCDP and Shadowgraphy.

Response: The response of these techniques for a finer spray (MVD 14.5 µm) and a coarser (MVD 33.8 µm) is understood from the bin-wise droplet counts and the corresponding cumulative mass fractions in the additional plot in Figure 9. The trend of the PSD for all the three methods is almost similar up to

50 µm, the FCDP measured count is in general almost an order higher than the PDI. Although only a few droplets above 30 µm are found with shadowgraphy, their weight is enough to deviate the cumulative mass curve from the others.
The droplet concentrations for FDCP and PDI are plotted in Figure 12. For the shadowgraphy technique, the droplet density is not obtained because of the difficulty in defining the probe volume. It can be seen that the FCDP gives slightly higher number concentrations The new plots are discussed in detail the manuscript.

The PDI measures LWC using eqn. 4, which proportional to the product of total drop concentration and corrected volume mean diameter. The manuscript should also show how LWC compares using this technique with LWC computed by integrating the complete PSD. The comparison should be shown as a function of MVD and drop concentration.
Response: This could be an additional interesting consideration. However, it would only broaden the knowledge about PDI. In contrast, the focus of the paper is on the comparison of measurement techniques rather than the detailed investigation of a single measurement technique. Therefore, we refrain from integrating the proposed tests for LWC calculation of the PDI into our investigation.
Furthermore, the LWC computed using equation 4 has shown a good agreement with the results of the WFR, so the manufacturer default (equation 4) seems suitable for our application.

The manuscript compares LWC measurements from the FCDP, PDI and RCT using the WFR as a standard. It is implied that LWC using WFR as a standard is very repeatable, on the order of 7%. In Section 4 a statement refers to Section 3 as justification for this, but far as I can tell in Section 3, this repeatability comes from the literature, not from actual tunnel tests. Yet, I assume there were LWC repeatability tests, similar to the MVD tests shown in Fig. 5, so please point out where I missed the LWC repeatability tests or include Figures showing results from them.
For all the experiments involving the LWC computation, the water flow rate is recorded and the corresponding LWC is computed. In total LWC from WFR is computed for more than 400 individual cases, of which several sets have been repeated to determine the variance of the water flow meters. The mean coefficient of variation of these repetitions is calculated to be 7% as reported in section 2.3.

Now, that said, based on the large amount of scatter shown in Figs. 12 – 14, either the tunnel flow characteristics or the measuring techniques, or both, appear to be contributing much more variability to LWC than the 20% Figure quoted in the text. It would be useful to show a complete uncertainty analysis for the WFR and test instruments measurements, but this is likely to be outside the scope of this paper. However, the manuscript should address tunnel and instrument LWC uncertainties in a more rigorous manner, not just quote the literature.
Indeed, a full uncertainty analysis based on the detection physics of each measurement technique is out of the scope of our manuscript. Nevertheless, we want to provide some estimates here. The uncertainties of the tunnel flow characteristics and the measurement techniques are both acting on the results presented in Figs. 13-15.

Let us therefore comment on the tunnel characteristics first. Here, the aerodynamic performance of the tunnel and the liquid atomizers that produce the droplet cloud need to be considered.

1) Aerodynamics: The repeatability of the wind tunnel and nozzle input conditions are studied and plotted in Figure 4 The precision limits for these variables for a sample run are also reported in section 2.3. The aero-thermal characteristics of the tunnel have already been calibrated as per the guidelines of SAE ARP 5905 with the recommended instruments and uncertainties which is now included in the manuscript. Thus, the temporal stability of the tunnel is guaranteed.

2) Liquid Atomizers: the repeatability of the spray can be appreciated from the plots in Figure 5. The temporal stability can be seen in Figure 6.

The atomization physics is highly dependent primarily on the supply pressures of water and air and the operating duty cycle. The fluctuations of these critical parameters lead to a higher uncertainty in the PSD and the LWC. To better estimate the uncertainty of the spray, additional data from another new spray system (not part of this manuscript) shall be mentioned here. The new system is equipped with a high accuracy Coriolis flow meter (accuracy 0.2%), the data was used to formulate an empirical form for the LWC (the variable being the input conditions to the nozzles), the 95% confidence interval of the model with the measurements is considered as the systematic bias of the model, the highest fluctuations of the pressure are considered as precision terms and the root-summed-squared (RSS) uncertainty computed over a wide range of operating conditions was found to be 0.045 g m^{-3}, yielding an total uncertainty of the spray LWC of 10%. This value is slightly higher than the repeatability characteristics, which are given by the coefficient of variation of 7% of the thermal mass flow meters used in the present study.
Given this tunnel operational constraint of creating an LWC with uncertainty of 10%, the fluctuations in Figs 13-15 beyond that value can be attributed to the uncertainties of the individual measurement techniques.
We mention these uncertainty considerations in Section 2.3 in the revised manuscript.

The sample conditions of these tests (droplet concentrations sometimes exceeding 2000 cm^{-3}) are typically only found in polluted environments. This, plus the slow droplet speed, limit the usefulness of the results of these experiments. These limitations need to be discussed in detail in the manuscript.
Response: It is true that the conditions used in this experiment only covers the lower boundary for what e.g. the FCDP is intended for, particle speed wise and at the same time uses large droplet number concentrations, which increases the likelihood of coincidence.
The wind tunnel is also for other applications than simulating flight conditions e.g. icing on wind turbine blades etc.
Nevertheless, the overall special conditions and limitations of the probes are going to be discussed in more detail in the new draft.

The poor sampling statistics for drop diameters > 30 microns (Figs 4 and 7) definitely introduce uncertainties in the LWC results that need to be addressed more rigorously.
Finally, it should be pointed out that without a rigorous uncertainty analysis of the absolute accuracy of the tunnel, all of the quoted accuracies are not absolute, but instead relative. That is, in addition to the random error associated with tunnel properties, there is some degree of undetermined bias error that is not considered. This needs to be emphasized in the manuscript, albeit, hints of this are included in some of the references cited.
Response: The higher bounds of the PSD for some conditions in BIWT can be approximated for example with a Langmuir D type distribution where D_{max} is 2.2·MVD. The expected D_{max} for the spray in Figure 3 (prev Fig .4) is 26.2 µm. The measurement shows droplets above 28 µm contribute less than 0.05% of the total volume agreeing with the expectated thus confirming the validty of the measurement. When the droplet count above 28 µm is doubled the change is in D_{30} is neglible from 9.38 µm to 9.48 µm that also results in negligible change in LWC. For this sample, the vicinity of 5.5 µm dominates the mass curve.
However, the presence of larger droplets in a small sample (1000 droplets) has a perceivable change in the MVD thus the D_{30} (Figure 6 right). As the sample size is increased (above 10000), the presence of the large droplets is reliably accounted and the uncertainity in MVD and D_{30} and LWC will be reduced as shown in Figure 6 left. Accordingly, all the PDI measurements are made with at least 20000 droplets per sample (for individual cases with low data rates at very low LWC) and in average approx.. 60000 droplets. With the FCDP the samples consist of at least 35000 droplets and in average of approx. 60000 droplets.

On the contrary, if the primary mode is not adequately sampled like the shadowgraphy data in Figure 9 left, any change in the count on the tail end of the distribution would alter the D30 and thus the LWC significantly. However, in the present paper, no LWC estimates are made from shadowgraphy.
The inherent complexity makes it impossible to derive a theoretical model for the PSD and lack of any other means in the present project to determine the actual PSD makes it difficult to quantify the bias. Albeit, the repeatability is higher as shown in Figure 5. Therefore, all of the measurements have some amount of unaccounted bias, but with a high precision thus a quality inter-comparison of the methods can be reliably made. These aspects are discussed explicitly in section 2.

Specific Comments:

1. Introduction
Page 2: When mentioning the cloud probes used by Ide (1999) and Cober et al. (2001), the manuscript should describe the resolution and size range of these probes so results can be compared with tunnel results.
Response: Ide (1999) performed the icing experiments in NASA IWT with MVD in the range 10 to 270 µm and velocities 22 to 112 m/s. LWC calculated by integrating the PSD spectra obtained from a combination of FSSP and OAP was reported to be significantly higher (1.2 to 2.7 times). than the LWC measured with icing blade an RCT. The large deviation was attribted to spectral broadening and coincidence errors. This is discussed in the manuscript in the introduction and in section 4.2.
The measurement ranges of the probes used by Cober et al. (2012) in the flight test campaign is also included in the manuscript.

2. Experimental Setup
Add a table (perhaps as a supplement) indicating the mean operating conditions for all of the data sets presented in this manuscript (Velocity, Temperature, RH, Air Pressure, Water Pressure, Water mass flow). This would be helpful to understand the scope of conditions for each type of drop measurement system. Also, list the number of data sets collected for each drop measurement technique (e.g., FCDP: 100 samples at 20 m s^{-1}, 200 samples at 30 m s^{-1}, 300 samples at 40 m s^{-1}).
Response: Certainly, this table would benefit in establishing the validity regions of these measurement and the degree of statistical reliability. The test conditions of all the runs are uploaded as a supplement and a short summary table is included in the paper.

Based on the data plotted in Fig. 11, it appears that the PDI datasets greatly exceed those of any other probe. This could be due to the high particle rejection rate and very low sample volume of the PDI. Please explain.
Response: LWC from WFR is computed for all the measurements along with PDI, FDCP and RCT and has therefore the largest number of measurements.
In this project PDI is used for reference calibration of the tunnel therefore more measurements are made with PDI. The reliability over a wide range of droplet sizes and the low acqisition time needed for a reliable sample enabled more than 300 measurements including repetitions.
On the other hand, due to the limited detectable droplet size range of FCDP and a limited time availability of the probe, only 34 valid LWC measurement were made with FCDP. Also, the measurements with RCT were limited to 37 different spray conditions due to the long measurement duration and the necessity to maintain extremely cold temperature (<-18°C).
The large disparity in number of measurements is purely from the above and not related to the low sample volume.

3.1. PDI

In this section it is noted that “The PVC has the greatest effect on the smallest size classes. Their influence on the LWC, on the other hand, is very small.” We have performed an independent analysis of the FCDP data set from this icing tunnel and determined that the peak of the particle mass size distribution is between 8µm and 10µm. Therefore in this study the vast majority of drops are very small (see PDI PSD in Figure 4 for confirmation where the mode is ~6 um). Given these concerns, the manuscript should include more details of the PDI small drop corrections and better quantify the errors. From Chuang et al 2008: "At very small droplet sizes, diffraction can become significant relative to refraction, and lead to oscillations in the φ versus d relationship at the smallest drop sizes, primarily in the size range below 4µm, but with some effects up to ~8µm."

Response: Thanks for invigorating our discussion on this aspect. This will be critical for extremely fine sprays where the mode is observed below 8 µm. The droplet size in PDI is obtained from the linear relations between the phase shift and size derived for a predominant reflection or refraction mode based on geometrical optics (Ofner 2001). Below 5 µm, the validity of the geometric optics tends to cease and the diffraction becomes significant leading to erroneous measurements if the linear relationships are used as mentioned in Chuang (2008). Bachalo and Sankar (1996) reported the uncertainty resulting from these oscillations to be under ±0.5 µm.

Chuang et al. propose using a large off axis angle for attaining higher accuracy of these small droplets but at the expense of the limiting the upper size. A discussion of the above is now included in the manuscript in chapter 4.1.

3.2. FCDP

The description of the FCDP sample volume is fairly convoluted. It is sufficiently described as SV=SA*TAS, where the SA is defined by calibration for a fixed qualification criteria. The SA is defined by laboratory calibration like that described in Faber et al. (2018). See the Table’s section of the review for more details.

Response: We agree that the description of the sample area can be facilitated.

In paragraph 3 it should be noted that the CDP and FCDP have similar operating principals, but the improved optics and electronics in FCDP allow for accurate sampling in higher particle concentrations (see comments on Table 2 below). The FCDP also differs from the older FSSP-100 probe in that the qualifier detector uses a slit aperture (200µm x 800µm), which was first introduced on the FSSP-300 probe with data described by Brenguier et al. (1998).

Response: We see that the FCDP is equipped with state of the art electronics and an advanced optics, compared to the CDP. When we reference system and operating specifics of the CDP, we do this as to show capabilities of an example for forward scattering spectrometer probes, without the intention to attribute its specifics to the FCDP. It is rather to put this measuring technique in general in comparison to the other techniques.

Furthermore comparable specific references solely applicable to the FCDP have not been found by the authors.

In the revised manuscript the difference between both systems, CDP and FCDP will be emphasized.

Lance et al. (2010) note that accurate sizing of the CDP instrument to ~200 cm^{-3} before being influenced by coincidence. However, improvements in the CDP (new limiting apertures) increased accuracy such that only 27% undercounting is estimated at concentrations of 500 cm-3 (Lance 2012). This level of uncertainty is still problematic. The FCDP was designed to incorporate the improvements of the CDP as well as reduce particle coincidence (the dominant source of error) by reducing the laser beam waist from 200µm to 80µm). Flight tests indicate reasonable agreement for LWC between the FCDP and hotwire probes for small droplet concentrations as high as ~1000 cm-3. The conditions in this study exceed these typical atmospheric conditions, so the FCDP uncertainty for these high drop concentrations range is not well described.

Response: In our citations we address mainly sources related to CDPs. So that repeated references to the (older) CDP are made throughout this chapter. A thorough comparison of both probes specifics and a comparison to other forward scatter cloud probes lies beyond the scope of this paper. But we agree that the major improvements of the FCDP versus the CDP, namely the electronics and optics should be addressed on the course of this chapter, especially when it comes to coincidence.
A usable citation, where confidence towards droplet concentration measurements ~1000cm-3 is expressed would be of help. The regime in which the FCDP is operated in this experiment will be discussed.

In paragraph 3, the authors cite up to a 50% uncertainty from Baumgardner 2017, but it should be noted that this quoted uncertainty (10 to 50% for light scattering probes), includes "Mie ambiguity, collection angles, coincidence, nonsphericity and shattering." In this study all droplets are assumed to be spherical, and shattering is minimal for the FCDP, so the 50% uncertainty does not apply here.
Response: It would be better to emphasize that the quoted citation from Baumgardner, 2017 is a maximum value for generic particle forward scattering probes, including all limitations for this measuring principle, including internal and external factors, which contribute to the cited up to 50% uncertainty. It is a good hint from the reviewer to elaborate the composition of the overall uncertainty and to point out what really applies for this probe and this experimental setup.

3.3. Shadowgraphy
Overall the Shadowgraphy technique is poorly described. More details of the instrument and post-processing are required such that the test could be replicated and verified by another group.
Response: The description is improved in chapter 3.3 with the details of the optics and light source. A description of the calibration is made. The DoF and border correction terms are discussed. Some recommendations are made from the experience. A description of the post processing is also made in the manuscript. The equipment specifications are also appended in the corresponding table 3.

In the last sentence from this section the data inter comparison is considered" almost identical." This statement requires quantification.
Response: In total 35 measurements are made with shadowgraphy, only 20 have individual conditions. The remaining15 are either repetitions or measurements with change in velocity for the same spray settings. Sixteen samples have MVD_{PDI} below 35 µm, which show the correlation of $MVD_{Shadow}=0.96 \cdot MVD_{PDI}$. The details on the measurement points are included in chapter 3.3 and the test matrix is added as a supplement.

3.4. Rotating Cylinder Technique
Stallabrass (1987) should be Stallabrass (1978)
Corrected

4.1. Repeatability
See General Comments.
The discussions of the wind tunnel temporal stability and its repeatability can be found in the new chapter 2.3. The analyses of the overall combined wind tunnel and measurement setup precision is now added at the end of each section in chapter 3.

Paragraph 2: "see section 4.1" within section 4.1, should be "see section 3.1".
Corrected
Paragraph 4: "see section 4.2" within section 4.1, should be "see section 3.2".
Corrected

4.2. Comparison

Paragraph 3: “A low sensitivity of the FCDP to larger particle sizes (> 30µm) may cause or contribute to the measured deviation of the FCDP with respect to the PDI for large droplets.” Is there evidence that the FCDP has a low sensitivity to larger drops? If so, provide a reference. The number of sampled drops is relatively low, due to the small sample volume and low concentration of larger drops, but this is true for all single-particle devices, including the PVI. Also, with long runs in an icing tunnel this should not be an issue, assuming the tunnel properties are repeatable, as claimed in Section 4.1.

Paragraph 3: “The transit time filter applied to the FCDP data during post-processing to reduce coincidence causes a rejection of droplets that have a too long transit time compared to the mean reverence [sic] velocity and thus reduces the droplet size spectrum evaluated as valid by large droplets.” Is there any evidence to support this assertion? If so, please provide the evidence, a reference, or sound physical explanation.

Response: In this case the authors refer to an effect not to be attributed to the FCDP probe itself, but to a slip of larger droplets within the airflow, compared to smaller droplets and the subsequent application of the transit time coincidence filter. Since droplet speed of larger droplets seem to be slightly lower than the airstream and in addition their sample number is overall fairly low, we have observed the tendency that the current transit time filtering for coincidence, based on the given TAS assumed as the particle airspeed, can lead to discarding of genuine counts of larger droplets, which deviate more than 25% from the C1C3 distribution, based on the given TAS.

Paragraph 5: “According to Lance et al. (2010), an additional source of error of the CDP might be the external geometry of the probe, which can alter the measured cloud particle size distribution.”

This statement does not apply to the FCDP because it has “anti-shattering tips” that minimize droplet splashing, whereas the CDP Lance used did not (at that time) have anti-shattering tips. The CDP can be equipped with anti-shattering tips now.

Response: We have to thank the reviewer for pointing out the fact that both CDP (in its initial design) and FCDP differ among other points in probe geometry. One major advantage of the FCDP’s shape is the application of anti-shattering tips. The challenge of droplet splashing is thus reduced. Nevertheless exposing in-situ probes into a droplet laden airstream alters the flow locally. As can be seen from the CFD-Simulation below and Spanu, et al. (2020), Weigl et al. (2016). When comparing different measuring techniques, this is an important factor to be mentioned, when discussing measurements.

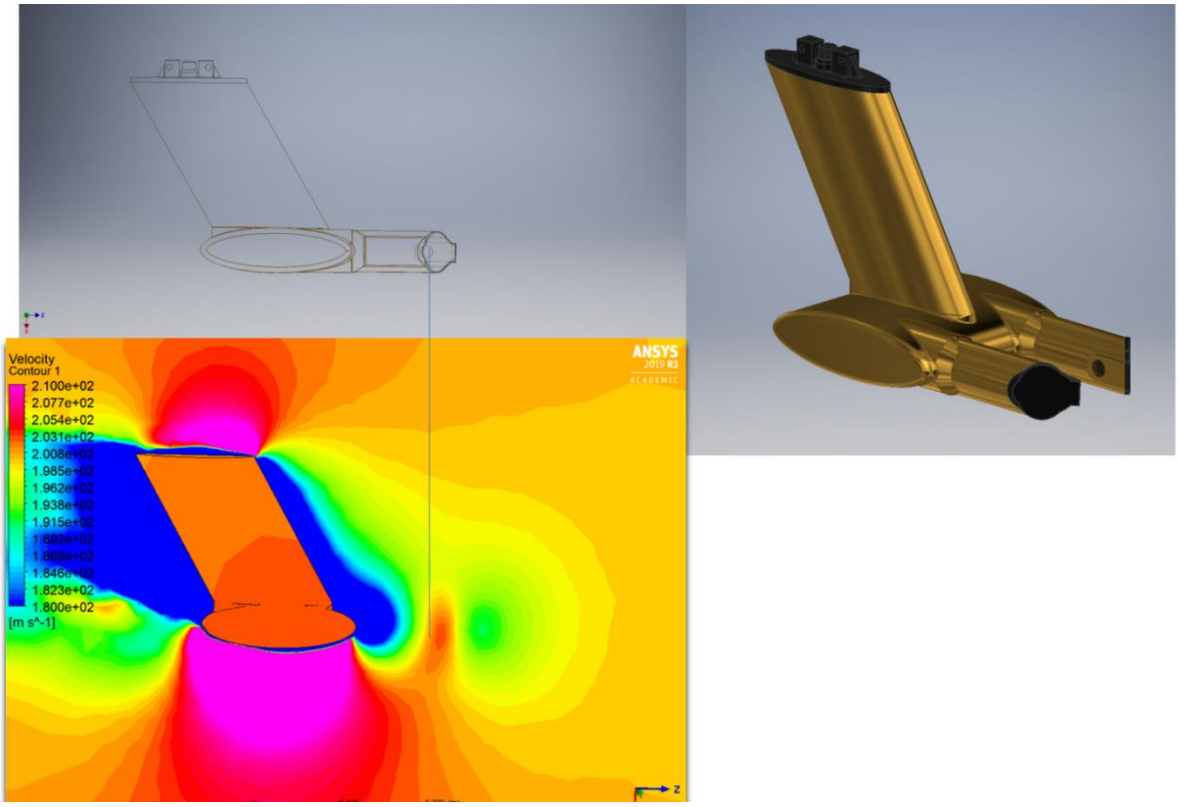

4.3. Comparison of LWC measurements
See General Comments, also:
Paragraph 6: "This can only be explained by higher particle number concentrations measured by the FCDP compared to the PDI."
Please provide particle concentrations and size distributions for the FCDP and PDI for the relevant wind tunnel datasets.
Response: The droplet number densities acquired by FCDP and PDI show a good agreement, that is shown in figure 12. In average the FCDP gives little higher concentrations than the PDI, what might be a possible explanation for the higher LWC results of the FCDP. The compared size distributions are shown in Figure 9. Both new figures are discussed in Chapter 4.1.

Following the example in Figure 7, the authors should indicate when the PDI and FCDP sampling statistics are poor (<100 particles per bin) and possibly remove these data from consideration.
Response: Our typical wind tunnel droplet size distribution has in almost all cases a long end with only very few large diameter droplets, as discussed in section 2.4. This can also be found in the literature (Rudoff et al., 1993; McDonell and Samuelsen, 1996). The number of particles per bin is as well a question of the bin size. In figure 7 we choose a bin width of 2µm. Increasing the bin width would automatically lead to higher droplet counts per bin. With a minimum droplet count of 10000 per measurement we present in the paper only measurement data with statistically secured MVD values.

5.0. Summary
Page 17 Paragraph 2: "The characterization of cloud droplet distributions with particle sizes > 100µm poses new challenges for droplet measurement techniques." Some Optical Array Probes are well suited to particle measurement in this range, specifically the 2D-S, which is commonly utilized for icing tunnel measurements of larger drops.
Response: Measurements with the 2D-S have already been carried out at TUBS IWT, in the size range from 10 to 1280µm (Bansmer et al. 2018). These comments were made in regard to the SLD icing conditions, where the LWC is around (0-1 0.4 g m^{-3}) with sizes often extending over 250µm.

The SLD clouds exhibit a bi-modal nature (Cober and Isac 2012) and the calibration of such a cloud in the wind tunnel requires to effectively capture the first mode (of small droplets) at 4-8µm as well as the second mode round 80-120µm. As discussed earlier the probes FCDP and FSSP have size limitations. Although shadowgraphy has no limitation on size simultaneously measuring both extremes of the SLD is highly challenging. The low LWC and broad spectrum of PSD of SLD conditions pose challenges for the individual measurement methods. Combinations like CCP, FSSP+OAP or others are to be employed. Although there are no such restrictions on PDI theoretically, the limited dynamic range and optimal selection of PMT voltage is difficult. Furthermore, the droplets in the cloud are sparse and gaining statistical confidence is more difficult than the conditions studied here.
This is briefly discussed in the revised manuscript.

References

Biter, C. J., et al., 1987: The drop-size response of the CSIRO liquid water probe. *J. Atmos. Oceanic Technol.* **4**, 359-367.
Response: Reference is now included in the manuscript.

Brenguier, Jean-Louis, et al., 1998: Improvements of droplet size distribution measurements with the Fast-FSSP (Forward Scattering Spectrometer Probe). *J. Atmos. Oceanic Technol.*, **15**, 1077-1090.
Response: Already cited, DOI link corrected

King, W. D., et al., 1985: Icing wind tunnel tests on the CSIRO liquid water probe. *J. Atmos. Oceanic Technol.*, **2**, 340-352.
Response: Already cited, DOI link corrected

Korolev, A., et al., 2013: Modification and tests of particle probe tips to mitigate effects of ice shattering. *J. Atmos. Oceanic Technol.*, **30**, 690-708.
Response: Reference is now included in the manuscript.

Lance, S., 2012: Coincidence errors in a cloud droplet probe (CDP) and a cloud and aerosol spectrometer (CAS), and the improved performance of a modified CDP. *J. Atmos. Oceanic Technol.*, **29**, 1532-1541.
Response: Reference is now included in the manuscript.

Strapp, J. W. and R.S. Schemenauer, 1982: Calibrations of Johnson-Williams Liquid Water Content Meters in a High-Speed Icing Tunnel. *J. Appl. Meteor.*, **21**, 98–108, https://doi.org/10.1175/1520-0450(1982)021<0098:COJWLW>2.0.CO;2
Response: Cited in the introduction

Figures

Figure 2: Add mean and variance values to each plot. It would also be helpful to add time-series data for the PDI, FCDP and Shadowgraphy (counts/sec or conc/sec). Perhaps it would be better to add the probes' time-series as a new Figure.
Response: We have added mean and standard variation in Figure 4. The water flow rate exhibits strong initial transient but stabilizes approximately after 15 seconds, this results in high variance in the water flow rate. A high precision, endurance and stability of other parameters can be appreciated from the low variance.

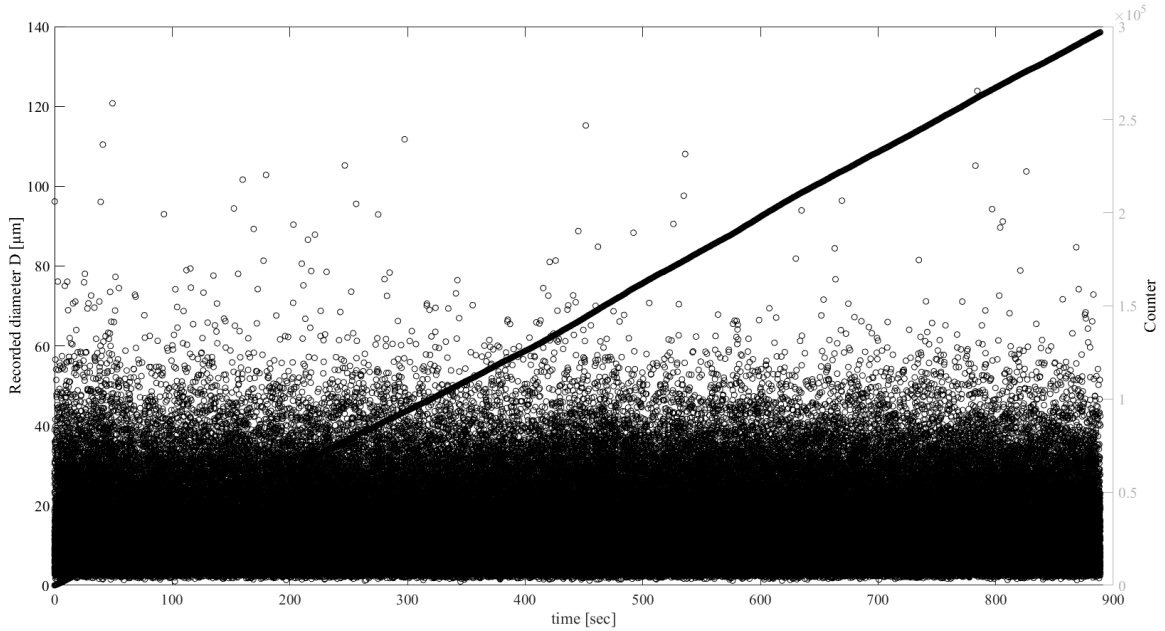

The time evolution of the droplet acquisition of PDI is plotted above, it can be seen that the data acquisition rate is fairly linear. Further the consistent pattern suggests two minutes should be long enough for a good measurement.
This Figure is not included in the manuscript. The temporal stability of the droplet cloud measured by the PDI can be seen in Figure 6 in the manuscript.

Figure 4: Add additional accumulated size distributions for the FCDP and Shadowgraphy. If possible, overlay distributions from all three methods on the same Figure indicating Concentration, LWC and MVD for each.
Response: We added a new figure (Figure 9) where we show and compare the accumulated size distributions of FCDP, PDI and Shadograhpy for two different droplet clouds.

Figure 5: Add R2 values.
Response: We calculated the correlation coefficients R^2 between all runs and added them in the caption of the figure to maintain the clear structure of the figure.
The high R^2 values show promising repeatability of the spray.

Figure 6: Based on the results in Figure 2, the conditions (Temp, RH) are not necessarily stable for the initial portion of the sample run. As such, it is hard to separate the MVD discrepancy as a function of true fluctuations vs counting statistics. Show size distributions for the initial 1000 droplets and the final 1000 droplets.
Response: The RH is initially unstable during start of test day, but over a few tests the tunnel will be saturated and can expect a stable humidity. We plotted the data for the initial 10000 and the final 10000 droplets in Figure 6 right and no large difference is found between them (overall 280000 droplets, duration 900 sec). This shows the temporal stability of the spray and complements the data in Figure 6.

Figure 7: This plot is very useful, but as with Figure 4 it should be amended to include lines for FCDP and Shadowgraphy. It may also be helpful to interpolate the higher resolution PDI data into the FCDP size bins for a more accurate comparison. Note that the FCDP size bins are chosen to smooth out Mie bumps and to improve sampling statistics for the larges drops. Add a dashed line to indicate the threshold for rejecting data due to inadequate data points in a bin (e.g., 100 counts bin-1).

Response: we have added a comparison of the droplet counts (fig. 12) as well as the relative cumulative volume curves in figure 9 for PDI, FCDP and Shadowgraphy.

Figure 9: These plots are useful, but additional plots should be added to show correlation with LWC and Concentration.
Response: The correlation of the LWC-ratio of the FCDP to the number concentration is shown in figure 15 right. We have additionally added a figure showing the number concentration from PDI and FCDP.

Figure 11: It hard to visually separate the WFR grey region from the PDI data points. Considering switching this plot to color or making individual scatter plots for PDI, FCDP and RCT
Response: We have changed plots to color.

Figure 14: Combine with Figure 12, and include sample plots for FCDP.
Response: We have combined the two plots and changed them to color.

Tables
Table 1: Include the model number of the PDI in the caption.
Response: The table is appended with additional important parameters

Table 2: Amend the table to include these values:
FCDP Beam Waist = 80µm
FCDP DOF Rejection Criteria = 0.9
FCDP Sample Area = 0.09mm^2
FCDP Size Range = 2-50µm
FCDP Serial number = 6
FCDP Calibration Date = 4/28/2017 (see sizing calibration curve below from manufacturer)

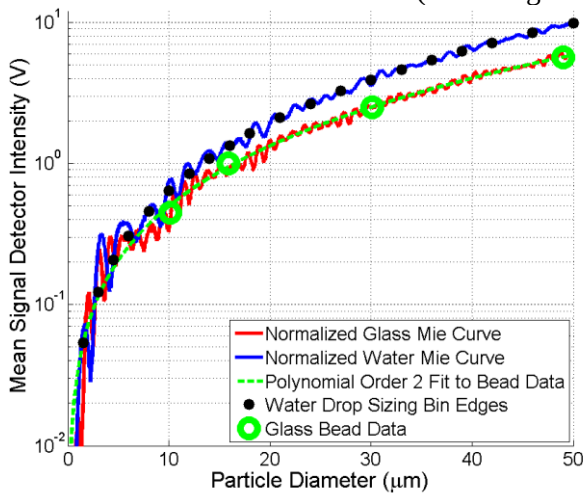

Response: thanks for sharing the data, appended the table

Table 3: Include details on the Shadowgraphy optical system similar to Table 1 for the PDI (wavelength, magnification, focal length, working distance, collection angle, etc.).
Response: Added details of the optics

Table 4: Define the table column variables in the caption.
Response: Changed the table to give a better overview and do not further use any variable names.

Response to the reviewer 2 of the manuscript: "Comparison of different droplet measurement techniques in the Braunschweig Icing Wind Tunnel" by Inken Knop et al.

General comments:

This technical paper reports on a wind tunnel experiment designed to compare several droplet measurement techniques. The experiment is conducted in the Braunschweig Icing Wind Tunnel where populations of supercooled droplets with size ranging from 1 to 150 µm are generated. The analysis focuses on Median Volumetric Diameter and Liquid Water Content, two key microphysical properties in the characterization of icing conditions.

The droplet measurement techniques involved, namely Phase Doppler Interferometry, shadowgraphy and FCDP, a commercial single particle counter, are commonly used by cloud physics and icing research groups. Nevertheless, there are still gaps in the understanding on their respective performances which is detrimental to the comparison of data produced by various research groups using different instruments. According to the authors, wind tunnel experiments offer a unique opportunity to test droplet measurement techniques in controlled and repeatable test conditions which in the end contributes to the
definition of measurement standards. Thus, the present study may bring some valuable contributions to the field and deserve a publication in AMT journal.
However, as highlighted in Kapulla et al. 2007, a thorough interpretation of the experimental results is necessary to draw a fair comparison between techniques based on different sizing and counting principles. In my opinion, this paper needs further elaboration regarding the presentation of the test conditions and the analysis of the data:

- The article does not contain a test matrix summarizing the experiment and providing the following information: wind tunnel settings (temperature, LWC, airspeed …), number of runs for each test conditions, duration and number of points collected by each probe in each run. The information scattered in the article indicates that several directions have been investigated (e.g. measurements in various wind tunnel conditions or influence of some probe settings) and that the analysis is based on a substantial number of data points, but it is hard to identify clearly the scope of this experiment and the statistical soundness of its results.

Response: A summary table of minimum and maximum test conditions for all the measurements is added in the manuscript and the total test matrix is added as supplemental material.

- MVD and LWC are inferred from particle size distributions (PSD) in all but two cases (rotating cylinder and tunnel air and water flow supply system settings). Given the importance of the measured PSD, the analysis given in section 4 should include a discussion on the PSD measured by the aforementioned techniques in the same test conditions. This would provide a solid basis for the subsequent interpretation of MVD and LWC results.

Response: The response of these techniques for a finer spray (MVD 14.5 µm) and a coarser (MVD 33.8 µm) is understood from the bin-wise droplet counts and the corresponding cumulative mass fractions in the additional plot in Figure 9. The trend of the PSD for all the three methods is almost similar up to 50 µm, the FCDP measured count is in general almost an order higher than the PDI. Although only a few droplets above 30 µm are found with shadowgraphy, their weight is enough to deviate the cumulative mass curve from the others.

In case of the FCDP microphysical properties of a spray such as MVD and LWC are higher order products derived from a sample statistics of droplet number and size. Uncertainties in the underlying measured parameter propagate, in the case of the LWC, with the order of three.

By constraining the FCDP's considered SA as a measure to constrain the measured droplet number and such the tendency for coincidence, decreases especially the counting statistics for larger droplets.

The droplet concentrations for FDCP and PDI are plotted in Figure 12. For the shadowgraphy technique, the droplet density is not obtained because of the difficulty in defining the probe volume. It can be seen that the FCDP and the PDI measurements give in most of the cases nearly the same number densities.

The new plots are discussed in the manuscript.

I strongly encourage the authors to deepen the analysis in order to strengthen their conclusions.
Response: We strived to deepen the analysis and some of the new items in the revision are below.

- The droplet spectrum, count and the droplet concentrations of the measurement systems are compared on a finer and coarser spray (Section 4.1).
- The repeatability of the spray is quantified and the temporal stability over small samples is presented (Section 2.3)
- An attempt is made to quantify the LWC uncertainty by analogies from a similar system. (Section 2.3)

Many changes are made to improve the readability and make the paper self-consistent.

Specific comments:
Abstract:
(general comment): could you state the range of conditions in which the presented results apply (at least a range of LWC and MVD and the type of shape/model characterizing the droplet size distributions generated at BIWT)
Response: The general valid range of MVD and LWC for this study in now listed in the abstract. Regarding the cloud distribution there is no specific regulatory requirement for the droplet size distribution of these fine sprays. Typical droplet size distributions of the BIWT are shown in fig. 3 and fig. 5. These can best be described by a Rossin-Rammler distribution. However, the description and investigation of different distribution functions is not the goal of this study.

l17-18: about the agreement of 15 % in MVD: the validity range of this results should be indicated. For instance, regarding shadowgraphy, your experiment shows that the indicated 15% are only valid for MVD< 35µm, see discussion in section 4.
Response: The stated agreement between these three measurements is for the range MVD=8-35µm. This is now included in the abstract. Due to the maximum detectable diameter of the FCDP of 50µm no measurements are discussed beyond this. The reasons for deviation of the shadowgraphy are discussed.

l21-22: (question) is it an agreement between the two techniques or an agreement of each of these techniques with the reference values calculated from the mass flow rate? In the first case, the result should be discussed in the paper in order to be included in the abstract. In the second case, the conclusion need to be rephrased, because it seems to contradict the results presented in fig. 11, on which a significant number of the PDI values fall outside the ±20% cone. From discussion in section 4.3, LWC from the PDI may only be within 20% of the reference values in 65% of the cases (97 out of 280 test points, as estimated from the data provided in section 4.3) or fall into 1:1 correlation with ±43% (whatever this means) in 91% of the cases.
Response: This is an agreement of each of these techniques with the reference values calculated from the mass flow rate. Accordingly, the quantities $|E_{PDI\,-\,WFR}|$ and $|E_{rotCyl\,-\,WFR}|$ are presented in the manuscript. The deviation is found to be higher at MVD of 35µm. The sentences in the abstract have been changed to correctly summarize the results of the LWC measurements.

Section 2:
(General comment): Add in this section a comprehensive description of your experiment. It could be test matrices summarizing the test points in terms of W/T settings and environmental conditions,

targeted MVD/LWC values, number of runs, duration and number of measurement points for each instrument.
Response: A summary table of tests maximum and minimum test conditions for the measurements is added in the manuscript and the total test matrix is added as supplemental material.

(Suggestion): To facilitate its readability, the section could be subdivided into three paragraphs: 2.1 Description of the experimental setup (already existing), 2.2 Presentation of the test conditions (new, test matrix) and 2.3 Assessment of repeatability (group together all the already existing pieces of information mentioned throughout the paper)
Response: Certainly, this improves the readability. The section is subdivided as follows:
2.1 Wind tunnel description
2.2 Parameters and Statistical Quantities for Comparison
2.3 Wind tunnel repeatability and uncertainty estimations
2.4 Test matrix

l109: (suggestion) provide the fluctuation level (0.1 bar) in relative units.
Response: The typical range of operating pressures is 2 to 5 bars, the 0,1bar fluctuation level is provided in %.

l127-128: “Here, we indicate the distributions and their fits in the respective experiment”: really good idea, but this has not been done, unfortunately.
Response: The description of the distribution and their possible fits would open a new chapter that is out of the scope of the actual paper. The misleading sentence was deleted.

l146: describe the test points and indicate the number of repetitions for each test point (use a test matrix for instance)
Response: There are several repetitions of the tests, 3 example cases with each of them with 3 repetitions are presented in figure 5. The test conditions of all compared tests can be found in the test matrix that will be uploaded as supplement material.

l147: regarding the repeatability: how do you calculate the “standard variation” for PSD? Is the standard variation equivalent to the coefficient of variation defined in equation 2?
l149: standard deviation (in g/m3) or coefficient of variation (in %)?
Response: The sentences have been corrected. It is the coefficient of variation of the MVD. We have additionally added R^2 values for the cases shown in figure 5.

(suggestion): as a complement to the comment l146, you could add a recap table (test matrix + table of results) containing test conditions, number of repetitions and statistical results (mean and standard deviation).
l159: include the test matrix here or in appendix. This is essential to give a comprehensive representation of the physical and statistical basis supporting this comparative study.
Response: We have added a summary table of the conducted experiments in the paper and will upload the full test matrix as a supplement.

l165: This might be really interesting for your instrument assessment, since the measurement results might depend on particular instrument settings. State for each instrument, what parameters were varied and what are the results and conclusions?

Response: the discussion of the different parameter settings of each technique are not part of the paper. Our focus is on the comparison of the measurement techniques not on the investigation of every single system. We forward the reader to a lot of literature where these investigations can be found.

Section 3:

l172: (general comment): can you indicate the general specifications of this instrument: size range (is it the static range in table 1?), velocity range, concentration range?

Response: We added some additional essential specifications of the instruments in the tables 1-3 and the comparable specifications in table 4.

l186: in table 1: can you indicate the two setups (manufacturer settings, McDonell and Samuelsen 1990) in two different columns for the sake of clarity?

Response: the two setups used, differ in the focal length of the transmitter and the dependent variables fringe spacing and beam waist at probe volume, that are mentioned in table 1 with a backslash.

l191: (question) Is 5 % related to the differences obtained by repeating the tests with different user controlled settings or is it just an indication of the repeatability of the PDI technique with McDonell and Samuelsen 1990 settings?

Response: the 5% value is the one obtained by McDonell and Samuelsen by their tests of the PDI sensitivity to user-controlled settings.

l192: D32 is not defined. Is it comparable to MVD? What point do you intend to make by quoting the results of McDonell and Samuelsen 1994? Equations (4) to (7): please make sure that each term in equations is properly defined (e.g. what is j in ttran(i,j)?), so that your article is self-consistent.

Response D32 is the Sauter mean Diameter: a representative number for the ratio of the volume to the surface area, often used in industrial spray applications. We decided to delete the sentence with the results of McDonell and Samuelsen 1994 since it is treating the D32 that we have not used in our study. We further added the definition of all terms used in our equations.

l200: The reference Zhu 1993 is not in the reference list

Response: There was a mistake in the year, we have corrected it

l228: The FCDP is not used in the experiment reported by Voigt et al. 2017. Please remove this reference.

Response: The reference has been removed.

l233: Do you use data of the 21st bin (over-size bin) in your calculation? Do you use a binning different than the default one set by the manufacturer?

Response: Here we quote the overall measuring capabilities specified by the manufacturer. For a data evaluation and further analysis we excluded the over-size bin. Information from this bin has been qualitatively recognized as a hint for the amount of droplets sensed beyond the actual size range. A droplet size calibration has been performed for the FCDP using borosilicate and soda lime glass beads. It was decided to stick with the manufacturer's bin setting from the probe checkout protocol, in order to allow for an impartialed bin assignment.

l235-236: Regarding uncertainty: when dealing with the FCDP, you assume implicitly that FCDP, CDP and even FSSP are truly equivalent, so that you can take conclusions derived from studies on FSSP/CDP

as granted for FCDP. Although all these probes use the same measurement principle (forward light scattering) and may share a similar optical layout, they differ in many aspects (e.g. the "novel fast electronics" highlighted l259). Can you provide references to studies demonstrating clearly the strict equivalence between FCDP and CDP/FSSP?
If there are no such references available, please make it clear when you discuss uncertainty that you are referring to studies on CDP/FSSP probes for lack of more relevant references. Then just mention the most relevant ones.
Response: We have to admit, that a more obvious distinction between the mentioned probes is favourable. To reference the FCDP to an FSSP and CDP might be misleading, without clearly stating its advantages. Due to a lack of a distinct study which directly compares CDP and FCDP, these probes specifics from FSSP and CDP have been employed.
The revised manuscript will point this out more clearly.

l241: The 32-34% accuracy range reported in Baumgardner 1983 is likely not applicable to your study ("old"FSSP with limited electronics).
Response: There is hardly any publication out there which explicitly gives an accuracy for forward scatter probes. The reviewer is totally right with her/his hint, that the quoted accuracy applies for early generation forward scatter probes.

l243: I think the CDP tested in Lance et al. 2010 differs from the FCDP you use handle coincidence quite differently.
Response: again it has to be brought to attention, that the quoted values only hold for a CDP, with an older optics and electronics.

l247: The content of table 2 and/or the description of the measurement protocol has to be expanded (see App. C in Lawson et al. 2017) based on your own data processing settings (e.g. what is set in the setup. m file, binning options). Also, please indicate your calibration protocol. (question): Does "DOF_crit = 0.9" mean that particles with Qual/Sig < 0.9 are discarded? How was the value (0.9) determined and did you assess the impact of this setting on MVD for instance?
Response:

FCDP SN	SN06
Calibration	as of 4/28/2017
DoF criteria:	Qual/Sig Ratio>= 0.9
SA	0.09mm²
Transit Time method	SPEC integrated Gaussian technique
Shattered particle filter	Arrival time algorithm

Operators manual are available on www.specinc.com/downloads. Matlab Software package FCDP_SP3C_V40 has been used for processing of raw files.

By selecting a Depth of Field criterion of Qual/Sig Ratio >=0.9 all droplet scatter events which do not meet this criterion are discarded. The size of the SA where droplets fulfil this respective criterion of >=0.9 has been determined within the scope of the probe calibration via a sensitivity area map using a droplet generator (Lance et al. 2010, Faber et al.,2018). A spatial resolution of this precision mapping has been 0.25mm along the laser beam direction and 0.03mm across the laser beam. Recorded particle by particle files that come with the newer electronics implemented in the FCDP, in contrast to the CDP, allows for a subsequent assignment of SA and DoFcrit pairs during post processing.
The realization of high droplet number concentrations and the increased possibility of coincidence urges the use of a high DoF ratio in order to target coincidence. The calibration specifies a DoF ratio of 0.9 as the peak value for this FCDP. SPEC recommends high DoF ratios also for accurate particle sizing.

l250-254: Could you be more precise in the description of the correction algorithms applied in post processing. For instance, the 125% threshold in beam transit time is not directly mentioned in any of the three papers you quote.

(question) How do you estimate the transit time vs drop size relationship? Do you comply with the "Half peak transit times versus size" procedure proposed in the FCDP post-processing manual?
Response: The initial step in order to reduce coincidence in high droplet number concentrations is to sharpen the DoF criterion. An additional filtering method to further reduces the influence of coincidence. SPEC provides a software module in Matlab (Vers10) with which the theoretical full peak transit time (TT) through a gaussian beam profile, depending on the droplet size and TAS can be fitted to the observed TT to size distribution from the measurement using the two fit parameter C1 and C3. Qualified scatter events that are outside the acceptance range, which is a deviation of more than 25% from this TT to size curve are regarded as coincident and are such discarded (SPEC inc. C1C3_V4 manual).

$$TT = \frac{2}{TAS}\sqrt{\mathrm{C1} * \log(\mathrm{D}^2) + \mathrm{C3}}$$

l260 (suggestion): this assertion needs to be quantified. It would make more sense to move it into section 4.
Response: Will be moved and discussed in section 4 as suggested

l277: can you indicate the "data rate" in table 3.
Response: The speed is essentially limited by the response of the camera in a single frame operation mode. The acquisition rate was 2.33 images per second. This is now mentioned in Shadowgraphy description in Chapter 3.3.

(general comment): Some of the "characteristic numbers" given in tables 1 - 3 are interesting, but it is hard to get a clear picture of the capacity of each setup due to the lack of common parameters. A recap table with comparable specifications such as size ranges, size resolution, sampled volume, concentration range, uncertainties, main characteristics and limitations … would be useful!
Response: We have added a table with the mean characteristics, together with the summary table of the conducted experiments.

l310-324: (suggestion) to be move to section 2 to establish the repeatability of the test conditions.
Response: We believe as WFR measurements itself is another measurement moving it will disturb the cohesion

l324: Can you provide quantitative estimates of the uncertainty in LWC derived from the wind tunnel settings (see also comment @l380)?
Response: The atomization physics of internal mixing nozzles are highly dependent on the supply pressures of water and air and the operating duty cycle. The fluctuations of these critical parameters lead to a higher uncertainty in the droplet sizes and the LWC, to some extent complemented by the uncertainties introduced by the wind tunnel performance.
The primary objective of this exercise is the probe inter-comparison for which the prerequisite is the repeatability or the reproducibility and the temporal stability. Accordingly, an emphasis is made on the repeatability of the wind tunnel and spray and an attempt is made to determine the uncertainty in LWC.

Firstly, the repeatability of the wind tunnel and nozzle input conditions are studied and plotted in figure 4. The precision limits for these variables for a sample run are also reported in section 2.3. The aero-thermal characteristics of the tunnel have already been calibrated according to the guidelines of SAE ARP 5905 with the recommended instruments and uncertainties which is now included in the manuscript. Thus the temporal stability of the tunnel is guaranteed.

Secondly, the repeatability of the spray can be appreciated from the plots in Figure 5.

To better estimate the uncertainty of the spray, additional data from another new spray system (not part of this manuscript) shall be mentioned here. The new system is equipped with a high accuracy Coriolis flow meter (accuracy 0.2%), the data was used to formulate an empirical form for the LWC (the variable being the input conditions to the nozzles), the 95% confidence interval of the model with the measurements is considered as the systematic bias of the model, the highest fluctuations of the pressure are considered as precision terms and the root-summed-squared (RSS) uncertainty computed over a wide range of operating conditions was found to be 0,045 g m^{-3}, yielding an total uncertainty of the spray LWC of 10%. This value is slightly higher than the repeatability characteristics, which are given by the coefficient of variation of 7% of the thermal mass flow meters used in the present study.
Given this tunnel operational constraint of creating an LWC with uncertainty of 10%, the fluctuations in Figs 14-16 beyond that value can be attributed to the uncertainties of the individual measurement techniques.
We will mention these uncertainty considerations in Section 2.3 in the revised manuscript.

section 4:
l330: to support this assertion, you can either show it analytically or quote Lance et al. 2010 (best).
Response: We have referred in the revised manuscript to Lance et al. 2010.

l332: (suggestion) I would remove this general statement drawn from Tropea 2011: it results from a broad overview of optical techniques and does not serve your work.
Response: We have removed the statement.

l334: about the title and the content of this section
(general comment) If we follow the logical construction of the paper, the repeatability of the test conditions is not a result, but a prerequisite for the comparison of measurement techniques. Since PDI is the reference method for assessing the repeatability of the test conditions, the discussion shall be moved in section 2.
Response: we agree with the comment and have shifted the investigations of the precision to the according sections in chapter 2.

(general comment): How do you define accuracy? In this study, “precision” sounds more appropriate than “accuracy”.
Response: Being a relative comparison with unaccounted biases it is appropriate to use precision instead of accuracy, changes are made wherever necessary.

l340: table 4: the test conditions and number of points underlying this table are not clearly stated. For instance: how is calculated the 5% value given in the cell (2,2)? I assume this is the mean value of an unknown series of coefficients of variation, each obtained from several repetitions made at the same test points, but it needs to be clarified (test matrix).
Response: The values of Table 4 are the mean values of the coefficients of variations, obtained from several repetitive measurements. This explanation is included at the beginning of chapter 3. The test matrixes of the repetitive measurements are also added as supplemental material.

l341: it is a good idea to assess the impact of the instrumental settings on the measured quantity. Please provide a detailed description of the setting being tested (test matrix…) and their impact on PSD or MVD/LWC.
l342-343: Unless the change in parameter settings is insignificant, it will make more sense to discuss separately the impact of different instrumental settings and the repeatability of the measurement techniques configured with “optimal” setting.

Response: the discussion of the different parameter settings of each technique are not part of the paper. Our focus is on the comparison of the measurement techniques not on the investigation of every single system. We forward the reader to a lot of literature where these investigations can be found.
A summary test matrix is now included in the manuscript and the detailed test matrix uploaded as supplemental material.

l357: “precision” rather than “accuracy”…
Response: has been replaced into “precision”

(question) For FCDP: did you investigate the impact of post-processing settings (inter arrival algorithm for instance) to retrieved PSD, as you did for the PDI?
Response: We have post processed the data under consideration of various filter techniques available in the Matlab postprocessing routine and assessed their influence on droplet number.
The inter arrival algorithm for instance was applied within the scope of a shattering filter. This filter has been applied although droplet number before and after was insensitive towards this inter arrival filter, which supports the conclusion that (maybe also caused by the presence of the anti shattering tips and with rather small droplets and no ice crystals) that shattering had no major role.
Additionally a variation of DoF criterion has been performed with 0.7 and mostly 0.8 and eventually 0.9.

l364-365: (suggestion) Are these two references useful here? 1) The argument is already given line 330 (Lance et al. 2010) and 2) neither Baumgardner 1983 nor Tropea 2011 are actually dealing with the FCDP.
Response: We agree, that this is a repetition of hinting towards the nature an error in LWC, when deriving it from droplet number and size. The subsequent references can be omitted.

l376-381: this should be in section 2, in which the repeatability of the test conditions is discussed. The calculation of LWC from the wind tunnel settings and its associated uncertainty shall be discussed all in the section (experimental setup).
Response: we agree with the comment and have shifted the investigations of the precision to the according sections in chapter 2.

l383-384: this assertion should be moved to section 3.1, in which the PDI measurement techniques are introduced.
Response: This has been moved and the advantages that make PDI more robust are discussed in section 3.1.

(Suggestion): is the reference to Basu et al. 2018 really relevant to this discussion? You’ve already provided enough convincing references related to the PDI measurement technique, while this one redirects the reader to a book dedicated in the first place to the physics of sprays for combustion and propulsion.
Response: the mentioned reference has been deleted.

l391: (question) is 14 % the largest relative difference found between FCDP and PDI MVD (marked measurement in fig 9 left) over the entire dataset (43 data points as estimated from fig 9)?
Response: The maximum difference in MVD is 14 % for all the 45 data points compared. The according sentence has been adapted in the manuscript.

l392: (question) why is 5 µm the lower limit for comparing FCDP and PDI spectra? From tables 1 and 2 both PDI and FCDP seems to measure below 5µm.
Response: The droplet size in PDI is obtained from the linear relations between the phase shift and size derived for a predominant reflection or refraction mode based on geometrical optics (Ofner 2001). Below 5 µm, the validity of the geometric optics tends to cease and the diffraction becomes significant leading to erroneous measurements if the linear relationships are used as mentioned in Chuang (2008). Bachalo and Sankar (1996) reported the uncertainty resulting from these oscillations to be under ±0.5 µm.
Chuang et al. propose using a large off axis angle for high accuracy of these small droplets but at the expense of the limiting the upper size.
A discussion of the above is included in the draft.

l396-397: "A low sensitivity of the FCDP to larger particle sizes (> 30 µm) ….the PDI for large droplets" : what makes you think that FCDP has a low sensitivity to particles larger than 30 µm? Is it a well-known behavior of the FCDP probe? If yes, could you provide references supporting this assertion?
Response: There are indeed hints of a lower sensitivity of the FCDP towards larger particles throughout various measurements, when comparing FCDP to CDP data e.g. ACTIVATE (current and ongoing NASA campaign) or in further wind tunnel tests with a FCDP, 2D-S combination at RTA, (Vienna, Austria) during the ICE GENESIS campaign. Unfortunately there is now reference available yet. A hint is available is the study by Thornberry et al. (2016), where the authors only use 12 size bins (out of the 21) up to only 24 µm for data evaluation. Larger sizes are covered by a 2D-S probe with a diode array resolution of 10 µm. Sizing (and imaging) capabilities of imager probes in this size range is subject to large errors (Baumgardner et al., (2017), …). Thornberry et al. (2016) even says while comparing the size range between 24µm-36µm of FCDP and 25µm-35µm of 2D-S respectively,

"This change (projected area of measured particles by 2D-S and FCDP) *in the relationship between the FCDP and 2-D-S is due to a greater decrease in the particle concentration measured by the FCDP in the 24–36 µm size range than that measured by the 2-D-S in the 25–35 µm bin."* So the change in his linear fit over the median projected area σ in FCDP measurements is attributed to a lower number concentration of larger particles >24µm compared to what the 2D-S has observed in the given size range.
But on the contrary Lawson et al. (2017) find a good agreement between the overlap region between FCDP and 2D-S.

Secondly, the argued velocity deficit for large droplets is hardly convincing: on fig 10 the density looks equally spread around unity for droplets below 50 µm (as far as I can see on my grey-printed scale picture).
Response: We compare velocity measurements from the PDI, a completely non-intrusive measuring technique, with an intrusive technique. With a surface area of the test section of 50cm x 50cm and a projected surface of the FCDP of approximately 171.69 cm² almost 7% ! of the cross sectional area are occupied by the probe itself, without taking a boundary layer within the test section into account (reducing the cross section by an assumed boundary layer thickness of 1cm yields a relative FCDP cover of 8%). Without assessing the stream lines around the FCDP and droplet trajectories in detail we might have to consider this effect, especially when comparing different measurement techniques. The figure below shows the velocity field across the centre plane through the SA, around a FCDP at a given true air speed of 200 m/s. Although our measurements were conducted at a lower TAS, we want to draw the attention towards the point that the velocity field along a potential particle trajectory ahead of the probe arms, as well as directly where the SA is located is modified by the probe itself. This fluid simulation was conducted in a free flow environment and without the constraint of a test section.

Velocity measurements with the PDI on the other hand are unobstructed and undisturbed by the probe itself.

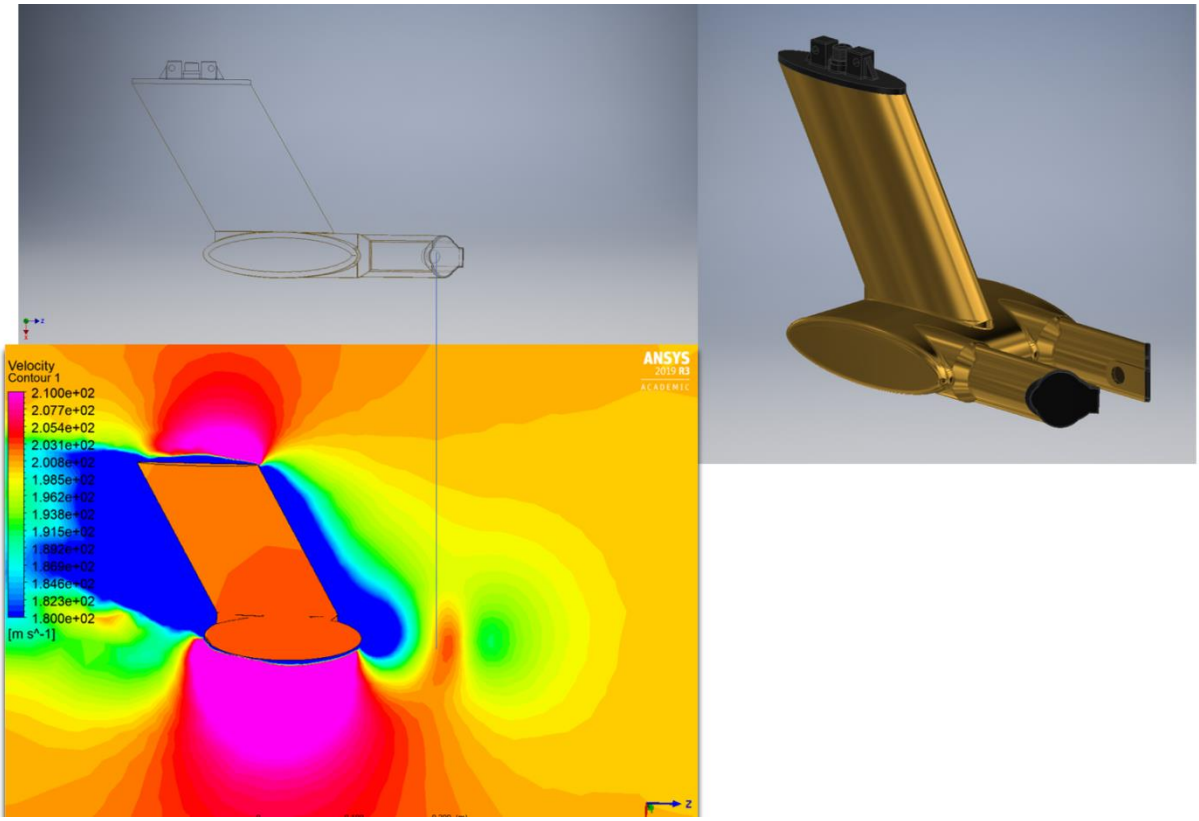

Simulated droplet speeds for this specific wind tunnel setup vary with droplet diameter. According to this simulation this effect is pronounced for larger droplets (>100µm).
Ansys simulation results for single droplets accelerated with the 3D-airflow of the wind tunnel nozzle show for droplets >150µm a velocity deficit of 10% in the test section.

Diameter in µm	simulated velocity at test section in ms^{-1}
160	36.07
200	34.86
240	33.73
280	32.73
320	31.92
360	31.36

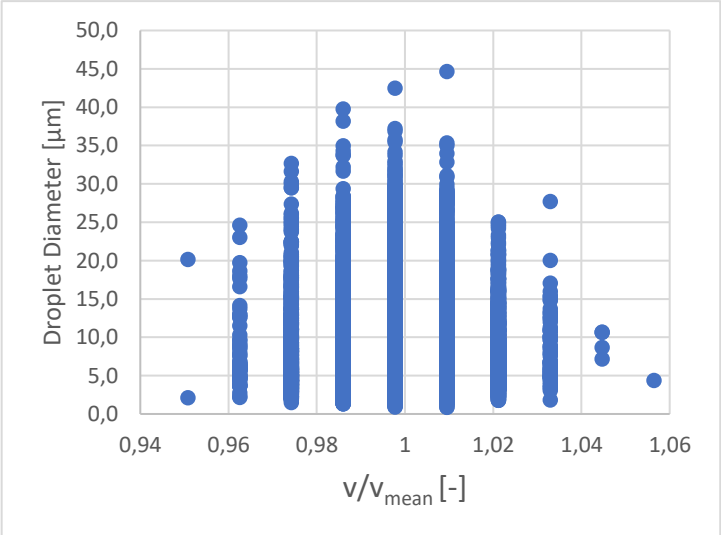

In addition to the particle velocity plot (figure 2) we show in the above image the PDI velocity measurement results of a test case with only small droplets. The maximal velocity deficit is less than 5%.

Finally, it would be really helpful for the reader to see how the PSD measured by PDI and FCDP differ, because at this point, one could argue that a lower MVD could either be caused by an overestimation

of the number of particles in the small size bins (e.g. due to shattering), or more likely an underestimation at large end of the spectra due to poor statistics in the large size bins, as it is argued.
Response (equal as above) : The response of these techniques for a finer spray (MVD 14.5 µm) and a coarser (MVD 33.8 µm) is understood from the bin-wise droplet counts and the corresponding cumulative mass fractions in the additional plot in Figure 9. The trend of the PSD for all the three methods is almost similar up to 50 µm, the FCDP measured count is in general almost an order higher than the PDI. Although only a few droplets above 30 µm are found with shadowgraphy, their weight is enough to deviate the cumulative mass curve from the others.
The droplet concentrations for FDCP and PDI is plotted in Figure 12. For the shadowgraphy technique, the droplet density is not obtained because of the difficulty in defining the probe volume. It can be seen that the FCDP and the PDI measurements give in most of the cases nearly the same number densities.
The new plots are discussed in the manuscript.

l400: Have you conducted a sensitivity study, where the transit time filter is changed, in order to reach this conclusion?
Response: Settings for the transit time filter have been adjusted throughout the whole data analysis process, until coming up with the current and final settings. The motivation for this proposed conclusion is the observation that the C1C3 fit routine has a good agreement along the maximum occurrence of observed transit time to droplet diameter pairs for smaller droplet sizes. Advancing to larger droplet sizes the gradient of the fitted theoretical transit time versus droplet size curve gradually deviates from observed transit times. This observation is so pronounced that larger droplets along the observed TT vs droplet diameter distribution might fall beyond the acceptance range of 125% about the fitted theoretical curve. This brought us to the proposed conclusion that particle speeds of larger droplets seem to deviate more from the theoretical TT vs diameter curve. This instance can be adjusted and was partially accounted for by manually shifting the fitted curve along the TT-axis (accepting potentially more coincident particles and allowing more larger droplets into the acceptance range). Although having observed the variation in particle speed with droplet size, this effect might not sufficiently explain the declining sensitivity with larger droplet diameter. It is more likely that the reduced sensitivity might be promoted by a statistical underrepresentation due to the strict DoF criterion and the corresponding small size of the SA. Thornberry et al.(2016) can be quoted as reference.

l403: The references “Lance et al. 2012” and “Lance et al. 2017” are missing in the reference list.
Response: Lance 2012 included, Reference “Lance et al. 2017” is a typo

l411: When you write “this effect can have a minor…”: have you actually assessed the effect of shattering, if any? A possibility would be to count the number of particles removed by the arrival time algorithm (provided you enable it during post-processing). The Spec software package v14 (old) contains a Quality Check program allowing to plot particle counts after the noise, shattering, DOF and TT qualification filters are applied. Such an analysis would be more convincing than the cited literature.
Response: The inter arrival algorithm for instance was applied within the scope of a shattering filter. This filter has been applied although droplet number before and after was insensitive towards this inter arrival filter, which supports the conclusion that (maybe also caused by the presence of the anti-shattering tips and with rather small droplets and no ice crystals) that shattering had no major role.

l411: The reference Weigel et al. 2017 is not in the reference list
Response: this reference will be added

l413: The ice accretion shown on figure 3 is quite impressive. Is it just an extreme case shown for illustration purposes? How much time does it take for this ice accretion to build up and how close is it to the sampling volume? Could you please comment on FCDP operation in such off-design conditions:

do you see variations in the measured size distributions as the ice shape grows? Do you discard data after some changes are noticed?
Response: Ice accretion in this extent as shown in figure 3 lead to an interruption of the current test point since its effect on the surrounding flow is not quantified. Furthermore probe icing of this extent also indicated icing on the flow guiding vanes of the recirculation wind tunnel. During these breaks ice build-ups have been mechanically removed and the current test point subsequently repeated. Ice-build ups of this extent have only been observed after several test points in a row, with a certain build-up time.

l416: the references to Faber et al. 2018 and Braga et al. 2017 may be misleading because neither PDI nor FCDP is included in these intercomparisons.
Response: We will search for another reference in order to assess the PDI measurements. Unfortunately to our knowledge there is no single reference which juxtaposes both instruments.

l422-423: Shadowgraphy instead of here? Could you double check the data
Response: we have corrected the sentences and checked the data in the revised manuscript.

l422-423: 8 measurement points (>35 µm, 20% of your 40-point dataset according to l278) have been excluded for being consistently different (systematic underestimation) from the expected values. Discussing the discrepancy in the PDI and shadowgraphy results found for MVD above 35µm, you suggest that a technical limitation of the shadowgraphy technique makes it unable to measure PSD correctly (insufficient statistical sampling) but your main conclusions (l18 and l510) assert that MVD measured by shadowgraphy and PDI lies within 15 %. Judging from the stated R^2 coefficient, I presume that the 15% value is only applicable if the 8 data points are discarded from the analysis. Therefore a caveat should clearly state that this is only true for MVD < 35 µm.
Response: Yes the best linear fit of $MVD_{Shadowgraphy}=0.97 \cdot MVD_{PDI}$ is obtained by excluding the data points above 35 µm. Now this caveat is made explicitly both in abstract and conclusion.

(s
uggestion): your experiment reveals a practical limitation of the shadowgraphy technique (at least when configured as in your experiment): this can be a valuable information for other W/T operators using this technique. Could you comment on whether or not this limitation is only applicable to your set up (low data rates, small field of view) or whether it is general to shadowgraphy (field of view against resolution dilemma, laser flashing rate limits) and what kind of modifications could be made to improve sizing and counting of log-normally distributed droplets from 1 to 150µm (e.g.: how to improve the data rates)?
Response: The low data rate of Shadowgraphy setup is primarily from the camera speed and the laser. A tradeoff has to be made on the size resolution of the droplet to be captured, it should be noted that the intensity of the light source reduces with the square of the magnification factor of the teleconvertors and it leads to a point where the gradients between the background and shadow become weak and the lower thresholds specified would lead to large noise picked as smaller droplet, further the resultant area reduction also reduces the probability of the finest droplets being detected thus hampering the quality of the measurement. Higher resolution cameras and high intensity light sources will improve a better.
A more detailed description of the Shadowgraphy setup is now included in the manuscript.

l428: Could you quantify “very low”? Data rate should be mentioned in table 3
Response: The data rate was approximately 2 frames per second. This is added in the description of the setup in Section 3.3.

l430 during the PDI-shadowgraphy results discussion. Are the MVD values calculated from PSD integrated over the 120 sec duration reported l258?

Response: the 120s duration was used for the FCDP measurements, since no online direct output of the counts is available. The MVD and LWC calculation was done over a time slot with temporal constant spray conditions (starting point of the evaluation after the ramp-up of the spray system). The FCDP samples consist thereby of at least 35000 droplets and in average of approx. 60000 droplets.
All the PDI measurements are made with at least 10000 droplets per sample. This led to a probe volume corrected total counts of 20000 for individual cases with low data rates at very low LWC and in average approx. 60000 counts, independent of the duration of the measurement. The MVD and LWC calculation was done over the entire data set, since the data recording was started always appr. 20s after the start of the spray system, so the ramp-up of the droplet cloud is not included in the results.
The Shadowgraphy measurements were done for at least 15 minutes to capture a minimum of 3000 droplets. This leads to more than 10000 counts with the applied DOF and border-correction. The data recording was started always appr. 20s after the start of the spray system, so the ramp-up of the droplet cloud in not included in the results.

l436-439: These general comments do not bring useful information at this point in the discussion. Suggestion to move these two sentences in section 3.
Response: The Sentences have been moved.

l468-469: "This can only be explained by higher particle number concentrations measured by the FCDP ":possibly yes, given that MVD from PDI and FCDP are very similar below 20µm. Please show the measured PSD for these test conditions.
Response: We have added a new figure (figure 9) to compare the PSD from the three measurement techniques and its discussion in the manuscript and as well the comparison of the measured particle concentrations of PDI and FCDP.

l466: what is the mean absolute value of the relative error between LWCFCDP and LWCWFR?
Response: As per the definition used in equation 3 it is 68,2%

l466: (general comment) It is surprising that an instrument which only detects particles over the first third of the total size distribution overestimates the LWC! According to fig 13 right, largest overestimations (of factor of two) are registered for small MVD values, in which case FCDP measurement should be in principle most accurate (particles within its measurement range). The quoted references report overestimations ranging from 20% (Faber et al. 2018) up to a factor of 4 (Rydblom et al. 2018). Your study could potentially bring new insights and precisions on this matter, provided that the analysis is deepened. The fact that the conclusions in Lance et al. 2010 are opposite to yours (l484) raises once again the question: how far should CDP and FCDP probes be considered equivalent? If probes are truly comparable, why do your study reaches the opposite conclusions?
Response: The FCDP's overestimation in LWC is promoted by high droplet number concentrations especially measured at small droplet sizes, as can be seen in the new Figures 9. Measuring conditions in the wind tunnel lie outside the customary environment in which the FCDP normally operates. References regarding FCDP's measuring capabilities are scarce.
The reference towards an opposite conclusion by Lance et al. (2010) was revised in the new Version of the manuscript and omitted. In detail Figure 7 in Lance et al. (2010) show a positive trend in LWC bias with increasing droplet number concentrations. Figure 15 shows simulated data where larger LWC biases are promoted by a high number concentration of small droplets rather than by larger droplets. Such a behavior indicates coincidence effects.

section 5:
l506: (suggestion) "test" instead of "boundary" conditions?
Response: It has been replaced

l509-510: The statement that the shadowgraphy values fall with 15% needs to be rephrased (range of validity, caveat about the low sampling rates, resolution vs sampling volume).
Response: It is revised with a caveat.

l512: "For the FCDP, the high sensitivity … (>35 µm) was **hypothesized**", rather than determined, since the discussion in its current state is hardly conclusive.
Response: It has been replaced

l515: (suggestion) this is an important conclusion but could you rephrase this, so that the limitation of your shadowgraphy setup appears clearly (low sampling rate more likely) and if possible, provide some piece of advice to others on how to improve the performance of the shadowgraphy technique in such test conditions.
Response: Improvements have been made in setup description and post processing description. Also some recommendation discussed previously are presented in section 3.3

l521: quantify "significantly"
Response: From figure 13 left it can be observed that LWC from FCDP varies by a factor of 0.5 to 3 of the LWC of WFR. Modified the lines to reflect the same.

page 29
Fig 10: Can you quantitatively comment the hypothesis made l95 about the drop velocity with respect to the air speed based on the PDI data collected in various test conditions?
Response: The velocity at the test section is computed with a computational model. At 40m/s of air speed, a 100 µm will be decelerated by the drag to a velocity of 37,8 m/s (5% deficit). As the droplet size decreases, the inertia of the droplet and the drag are negligible and therefore will have the same velocity as the surrounding air all along its path from injection to the test section. Accordingly, with tunnel fluctuations (±1,5%) and measurement errors, the smaller particle are expected to have a large band of normalized velocities, the same is being reflected in PDI. Larger particles have higher inertia and little less sensitivity to instantaneous fluctuation in the tunnel and also experience considerable drag that causes velocity deficit (5% for 100 µm) this demonstrates the consistency and robustness of PDI for velocity measurement.

Technical corrections (compact listing of purely technical corrections, typing errors)
Response: All of the typing errors are fixed

l52: Similarly, to the experiments conducted here, Ide (1999) compared: first comma to be deleted
l345: is the reference to section 4.1 correct or should it be section 3.1?
l401: reference instead of reverence
l476: LWCWFR rather than LWCPDI. This typo error prompt me to ask whether or not "PDI" was meant l468 since the comparison is made with WFR in the first place?
l498: **t**he instead of The
l505/506: a good repeatability **of/?** the MVD… (word missing)

Comparison of different droplet measurement techniques in the Braunschweig Icing Wind Tunnel

Inken Knop[1], Stephan Bansmer[1], Valerian Hahn[2,3], Christiane Voigt[2,3]

[1]Institute of Fluid Mechanics, Technische Universität Braunschweig, 38108 Braunschweig, Germany

[2]Deutsches Zentrum für Luft- und Raumfahrt (DLR), Institute of Atmospheric Physics, 82234 Wessling, Germany

[3]Institute of Atmospheric Physics, University Mainz, 55881 Mainz, Germany

Correspondence to: Inken Knop (i.knop@tu-braunschweig.de)

Abstract. The generation, transport and characterisation of supercooled droplets in multiphase wind tunnel-test facilities is of great importance for conducting icing experiments and to better understand cloud microphysical processes such as coalescence, ice nucleation, accretion and riming. To this end, a spray system has been developed, tested and calibrated in the Braunschweig Icing Wind Tunnel. Liquid droplets in the size range of 1 to 150 µm produced by pneumatic atomizers were accelerated to velocities between 10 and 40 m s^{-1} and supercooled to temperatures between 0 and -20 °C. Thereby, liquid water contents between 0.07 and 2.5 g m^{-3} were obtained in the test section. The wind tunnel conditions were stable and reproducible within 3% standard variation for median volumetric diameter (MVD) and 7% standard deviation for liquid water content (LWC). Different instruments were integrated in the icing wind tunnel measuring the particle size distribution (PSD), MVD and LWC. Phase Doppler Interferometry (PDI), laser spectroscopy with a Fast Cloud Droplet Probe (FCDP) and shadowgraphy were systematically compared for present wind tunnel conditions. MVDs measured with the three instruments agreed within 15% in the range between 8 µm and 35 µm, and showed high coefficients of determination (R^2) of 0.985 for FCDP and 0.799 for shadowgraphy with respect to PDI data. Between 35 and 56 µm MVD, the shadowgraphy data exhibit a low bias with respect to PDI. The instruments' trends and biases for selected droplet conditions are discussed. LWCs determined from mass flow calculations in the range 0.07 – 1.5 g m^{-3} are compared to measurements of the bulk phase rotating cylinder technique (RCT) and the above mentioned single particle instruments. For RCT, agreement to the mass flow calculations of approximately 20% in LWC was achieved. For PDI 84% of measurement points with LWC < 0.5 g m^{-3} agree to mass flow calculations within a range of ± 0.1 g m^{-3}. Using the different techniques, a comprehensive wind tunnel calibration for supercooled droplets was achieved, which is a prerequisite to provide well characterized liquid cloud conditions for icing tests for aerospace, wind turbines and power networks.

1 Introduction

Supercooled water droplets cause icing of aircraft (Poots et al., 2000), helicopters (Kreeger et al., 2015), wind turbines (Battisti, 2015), and power networks (Farzaneh, 2008). As numerical icing codes are now widely used in the design and certification stages, the need for reliable experimental validation increases. The precise detection of the microphysical particle properties and the liquid water content (LWC) of droplet distributions produced by spray systems in wind tunnel test facilities thereby is of great importance to improve ice accretion models. Besides icing research, other technical applications of spray systems, such as fuel sprays (Bossard and Peck, 1996), agricultural sprays (Tuck et al., 1997), or spray painting (Snyder et al., 1989), are of interest for related industry and research.

Various measurement techniques that differ in terms of the underlying physical principles and the probe design are currently used to characterize droplet clouds. One way to classify these is the differentiation between integrating systems investigating liquid clouds as entities and single-particle instruments (Brenguier et al., 1998). Another possible criterion distinguishes between intrusive and non-intrusive systems (Tropea, 2011). Three types of measurement techniques allow to measure the total mass of an ensemble of liquid droplets: systems that calculate the LWC on the basis of single droplet size measurements (e.g., Fast Cloud Droplet Probe (FCDP), Phase Doppler Interferometry (PDI)), hot-wire methods (e.g., King LWC probe, Nevzorov probe), and ice accretion methods (e.g., rotating cylinder technique (RCT), icing blade) (Ide, 1999). A comprehensive overview of available techniques for cloud measurements is given by Baumgardner et al. (2017) including results from previous methodological papers (Tropea, 2011; Fansler and Parrish, 2015; Linne, 2013).

There are numerous icing wind tunnels worldwide that were used for intercomparison of droplet measurement techniques in the past, including the NASA Glenn Research Center Icing Tunnel (Ide and Oldenburg, 2001) and the Altitude Icing Wind Tunnel of the National Research Council of Canada (Strapp and Schemenauer, 1982). Here we show results from droplet measurements performed in the Braunschweig Icing Wind Tunnel (BIWT) (Bansmer et al., 2018) initially designed to provide large supercooled droplets (median volumetric diameter (MVD) ≈ 80µm) and ice particles for icing experiments in mixed phase and ice crystal conditions. In 2016 the wind tunnel has been further upgraded to introduce also small liquid droplets, relevant e.g. for research on wind turbine icing and Appendix C (MVD <50 µm, FAA) inflight icing conditions. During the extensive calibration of the new spray system different measurement techniques were integrated into the wind tunnel to measure the particle size distribution (PSD) and the LWC. Measurements of the PSD of liquid particle ensembles with droplet sizes < 150 µm were performed with the PDI, the FCDP and shadowgraphy and results are compared within the instrumental measurement ranges. In addition, the LWC detected with the PDI, the FCDP, and the RCT are compared and related to LWC calculations, based on injected water mass flow and wind tunnel flow velocity. Thereby the laboratory environment of the wind tunnel provides a homogenous ensemble of water droplets at a given constant target speed.

Similar to the experiments conducted here, Ide (1999) compared different LWC measurement techniques in the NASA Glenn Research Center Icing Tunnel with spray MVD in the range 10 to 270 µm and velocities 22 to 112 m s^{-1}. The instruments tested in 1999 were the icing blade, a single rotating cylinder, the Johnson-Williams and CSIRO-King hot-wire probes, the Nevzorov LWC/TWC (Total Water Content) probe and the LWC calculated from the combined droplet distributions of two droplet sizing probes – the FSSP (range 2 -47 µm) and the Optical Array Probe (range 15-450 µm) OAP Particle Measuring Systems, Inc. of Boulder, Colorado. The LWC calculated from the droplet distributions measured with OAP and FSSP was found to be overestimated. Cober et al. (2012) published a comparison of different LWC measurement techniques for large supercooled droplets in flight tests. They evaluated a Rosemount icing detector from Goodrich Corporation, which can measure the LWC when environmental conditions lead to a temperature below the Ludlam limit. Furthermore, two FSSP and three different 2D-imaging systems FSSP (3-45 µm and 5-95 µm), 2D-C (25-800 µm), 2D-G (25-1600 µm), 2D-P (20-6400 µm), were installed during their cloud research flights. Later on, the results of these publications are used for comparison purposes.

This paper describes the experimental setup of the BIWT, the new designed spray system and its performance. After the description of the individual measurement techniques, results for MVD and LWC are discussed in sight of the different measurement methods. The outlook presents a short summary, future research topics and plans for a second update of the spray system to generate bimodal PSDs.

2 Experimental Setup

The following chapter contains some basic information regarding the wind tunnel setup, experimental boundary conditions and statistical estimators to evaluate our results. Furthermore, the repeatability of the wind tunnel for the aerothermal behavior as well as the droplet cloud will be presented with example test cases. The design of the test matrix will be discussed at the end of the chapter.

2.1 Wind Tunnel Description

The BIWT is a state-of-the-art academic research facility that complies with the SAE ARP5905 requirements and has been actively engaged in several international projects in collaboration with multiple aerospace agencies and industries. A detailed overview of the BIWT is given by Bansmer et al. (2018). The basic design is a closed-loop wind tunnel with a 0.5 m x 0.5 m cross-sectional area at the test section with adjustable velocities between 10 and 40 m s^{-1}. The static air temperature can be controlled between -25 °C and +30 °C. In addition to the injection of water droplets through a spray system, it is also possible to introduce a cloud of ice particles to simulate different conditions of atmospheric icing in the test section. The BIWT is not pressurized and yields Reynolds numbers up to $2 \cdot 10^6$ at its full speed. To further extend the operational envelope of the tunnel, numerous scaling methods based on similitude of geometry, droplet trajectories and the impingement heat transfer are available. A comprehensive description of the scaling methods can be found in Anderson (2004). In the present study, we do not apply any scaling to the results in order to avoid introducing additional sources of uncertainty to our results.
The spray system of the tunnel consists of 30 pulsed air-assist atomizers (see Fig. 1) from Spraying Systems Co (PulsaJet AB10000JJAU) with fluid cap PFJ-08-50 (diameter of the final liquid discharge orifice 0.2 mm) and air cap PAJ-73-1-60 (diameter of the final orifice outlet of 1.5 mm). The general random nature of the atomization process results in sprays with a wide spectrum of droplet sizes with the mean value depending on the supply pressure (Lefebvre and McDonell, 2017). The electrically-actuated atomizers are controlled by the AutoJet Spray Controller. The pulse width modulated (PWM) flow control enables an independent change of liquid mass flow at constant supply pressure (and therefore a relatively constant droplet size). The atomizers are switched on and off up to 10000 times a minute, making the spray appear constant for the purpose of icing research. Furthermore, the electrically-actuated spray nozzles are closed if not in use, even if the system is already pressurized. This leads to a smaller delay from starting the spray to steady-state condition of the fully developed droplet size distribution. Demineralized water is used for droplet generation with a very low level of contamination to avoid clogging of the spray nozzles and freezing out of the droplets in the cold airflow. All components of the supply structure outside the tunnel were chosen with regard to small pressure losses and compatibility of materials for the demineralized water. Separate valves for every spray bar enable a selective usage of only a specific part of the atomizers. A separate management system to control every atomizer individually has been implemented to turn off specific atomizers (e.g., in the case of low flow velocities and high probability of icing of the wind tunnel

walls, the spray atomizers near the wind tunnel walls can be stopped). Thermal volume flowmeters measure the averaged water flow rate for each spray bar, thus providing a hint when nozzles clog or freeze over. The actuation of the electrically controlled pressure regulators for the water and the compressed air, all valves, and the control unit of the PWM-flow system are integrated into the wind tunnel software, providing the user with remote control of the whole spray system. All aerothermal characteristics, like airflow uniformity, turbulence intensity, and total temperature of the wind tunnel flow, comply with SAE ARP5905 specifications (Bansmer et al., 2018).

The droplet measurements were conducted along the centerline in the wind tunnel test section 4 m downstream from the spray system. The bluff body shape of the spray bars (see Fig. 1) promotes a homogenous spatial dispersion of droplets in the airflow. It has been shown numerically that droplets up to a diameter of 100 µm have almost no slip to the wind tunnel speed (Bansmer et al., 2018), leading to the assumption that the droplet velocity in the test section agrees well with the adjusted air speed. The hypothesis is supported by an example PDI dataset shown in Fig. 2 (Fig. 2 is further discussed in Section 4.1). With an uncertainty of 0.5 m s^{-1} and a most likely negative slip for large droplets the data of the example test case shows a good agreement between wind tunnel and droplet velocity.

2.2 Parameters and Statistical Quantities for Comparison

Procedures for determining appropriate sample size, size class widths, and characteristic droplet sizes for the characterization of sprays were applied according to ASTM E799-03 (Practice for Determining Data Criteria and Processing for Liquid Drop Size Analysis). In icing research, the histogram of the number of droplets with diameters between D ± ΔD/2 is used most frequently, together with cumulative curves of the liquid cloud volume. In this study, the characteristic diameters of the cumulative volume curve like the MVD (or DV0.5) and the 10 and 90 percentiles (DV0.1 and DV0.9) are used to describe the droplet distributions as shown in Fig. 3 for a test delivering a cloud ensemble with an MVD of 11.8 µm. Droplet distributions in the atmosphere typically follow a log-normal behaviour (Langmuir and Blodgett, 1961). The atomization of fluids in laboratory setups may lead to different particle size distributions such as normal, Nukiyama–Tanasawa, Rosin–Rammler, modified Rosin-Rammler, and upper-limit distributions (Lefebvre and McDonell, 2017).

Another important variable for icing research is the already mentioned LWC, which represents the mixing of the available mass of water within a defined air volume:

$$LWC = \frac{m_{Water}}{V_{air}} \tag{1}$$

The repeatability of measurements is characterized based on the coefficient of variation (i.e., the standard deviations over several repeated measurements normalized by the mean values):

$$\sigma = \frac{1}{\overline{MVD}} \sqrt{\frac{\sum(MVD-\overline{MVD})^2}{n}} \tag{2}$$

To describe the consistency of the results from different measurement techniques, we use the mean absolute value of the relative error. Therefore, the sum over all differences in the value of interest between the considered and the reference technique, normalized by the reference value, is divided by the number of comparable measurements. The absolute value of the difference avoids a cancellation of positive and negative errors.

$$|E_{MVD}| = \frac{1}{n} \sum \frac{|MVD_{compare} - MVD_{PDI}|}{MVD_{PDI}} \tag{3}$$

2.3 Wind Tunnel Repeatability and Uncertainty Estimations

For the analysis of wind tunnel repeatability and an uncertainty estimation, the pure aerodynamic performance of the tunnel and the stability of the liquid atomizers that produce the droplet cloud need to be considered.

Regarding the aerodynamic repeatability, temperature and airspeed of the flow can be regulated with the required accuracy according to SAE ARP5905, however, the humidity and static pressure cannot. The static pressure in the test section is hence dependent on the ambient pressure, whereas the humidity in the test section is governed by the duration of water injection. The relative humidity of the two-phase flow quickly increased after the first few tests at the beginning of a measurement day to > 90%.

For a better description of the temporal stability of the wind tunnel and spray system test conditions, Fig. 4 shows a representative 15-minute test record. The upper three diagrams describe the quality of the wind tunnel flow and the lower three diagrams the spray system. All measured flow quality parameters meet the requirements of the SAE ARP5905 for the temporal stability along the tunnel centerline and thereby the measurement positions of the intercomparison tests: The flow velocity fluctuates by a maximum of 1.6%. The tunnel temperature varies by less than 0.5 °C and the relative humidity, as the only non-adjustable variable, varies by max. 1.5% over a time period of 15 minutes. The SAE ARP5905 allowable deviation criteria for the velocity and temperature being ±2% and ±0.5°C respectively measured with instruments having an uncertainty range of ±1% and ±0.5°C. The precision limits of velocity and temperature are computed for a sample run as defined in Coleman and Steele (1995) and AGARD-AR-304. Their values lower than 0.01 indicate negligible temporal fluctuations in the aerodynamic performance of the tunnel.

Next, the stability of the liquid atomization is considered. The constant supply system parameters are a prerequisite for a temporally constant atomization process and thus a temporally constant droplet cloud in the test section. By monitoring the water mass flow, it can be determined that, despite previous pressurization of the pipes, approx. 15 seconds are required until the volume flow stabilizes. Thereafter, air and water pressures fluctuate in the supply system of the spray atomizers on average by 0.04 bar (3%) and 0.03 bar (1%), respectively. To estimate the influence of these fluctuations on the water flow rate, a similar spraying system with a different air cap is used that incorporates a high accuracy Coriolis flow meter (manufacturer specified accuracy 0.2%). A parametric model for LWC is developed using the pressure fluctuations as input and the Coriolis flow meter data as output. Performing an uncertainty propagation analysis and assuming a 95% confidence interval, the root of the sum of the squares (RSS) uncertainty bounds of the LWC can be conservatively considered to be within the 10% limit.

In the BIWT setup the water volume flow is measured with one thermal volumetric flow meter per row of six atomizers. Due to the very low total water volume flow through every thermal volumetric flow meter (down to less than 10 ml min^{-1} per row) and the pulsation of the nozzles, the uncertainty of the volume flow measurement is approximately 20%.

For the evaluation of the deviations between the different measuring techniques, an investigation of the repeatability of the droplet cloud in the wind tunnel is needed. Due to the afore mentioned small pressure fluctuations in the supply system and slight fluctuations in the wind tunnel velocity, minor variations in the droplet size distribution and the LWC may occur even with the same settings for all wind tunnel parameters. In addition, there is the non-deterministic atomization process at the pneumatic atomizers themselves (Liu et al., 2005) leading to small temporal variations in the droplet cloud. To determine the size of these variations for the MVD in the BIWT reference measurements have been performed with the PDI and selected measurement points have been

repeated with exactly the same experimental setup. The results of some of these tests are shown in Fig. 5. The repeatability of MVD shows a coefficient of variation of ± 3%, including uncertainties in the wind tunnel and the measurement setup.

To again underline the good temporal stability of the spray system, the PSD and corresponding cumulative mass fractions for the first 1000, middle 1000 and last 1000 droplets of a 15 minutes long single PDI measurement are plotted in Fig. 6 (right). The average acquisition rate of the measurement was 338 droplets per second. The PSDs agree very well with each other, except those of the first 1000 droplets. This is due to the transient behaviour in the first seconds of the spray ramp-up, where the atomization has not stabilized yet, what can be also seen in the water mass flow in Fig. 4.

The inherent complex interactions in the spray process makes it challenging to obtain the actual value of the distribution, therefore the uncertainty bounds of the spray were not ascertained in the present study. The high R^2 values in Fig. 5 indicate a promising repeatability of the spray system, facilitating a reliable relative comparison of PDI, FCDP and shadowgraphy. For the test points shown in Fig. 5, the LWC based on the water mass flow was also investigated. This resulted in a coefficient of variation of the LWC in repeated measurements of 7%, indicating altogether a good repeatability of the wind tunnel conditions with respect to particle size and LWC. The afore mentioned value of the RSS uncertainty bounds is slightly higher than the LWC repeatability characteristics, which are given by the coefficient of variation of 7% of the thermal mass flow meters used in the present study, and can be explained by the unsteadiness of the atomization process.

2.4 Test Matrix

The test matrix for the measurements was designed to test each independent variable separately. To this end, the droplet diameters were first varied using different combinations of air and water pressure. During these tests the duty cycle of the nozzles and the velocity and temperature of the tunnel were not changed. Then, the duty cycle was varied for selected pressure combinations in order to classify its influence on the MVD and LWC. Furthermore, the flow velocity was changed from 10 up to 40 m s^{-1} with exactly the same spray system settings, which should lead only to changes in LWC. Finally, the temperature was varied, which theoretically should neither have a noticeable influence on the droplet size nor the LWC. In addition, some parameters of every measurement technique were varied depending on the individual system. These tests were not further discussed here, since the investigations of the techniques themselves have been widely done in literature (see Section 3). Overall, the comparison is made for sprays in the MVD range of 8 to 56 µm (PDI size being the reference) and corresponding LWC from 0.07 – 2.5 g m^{-3} (reference LWC from water flow rate). The here tested measurement ranges as well as some comparable key parameters of the different measurement techniques are summarized in Table 4. The detailed test conditions for the comparison of the MVD and LWC can be found in the supplementary material.

Shadowgraphy, PDI, and FCDP measurements of droplet PSDs and LWC were performed in test campaigns in 2017 and some PDI measurements were repeated in 2019. The RCT measurements were performed in summer 2018. The static pressure in the test section varied during these measurements between 990 hPa and 1007 hPa. Most of the shadowgraphy, PDI and FCDP experiments were conducted at -5°C to avoid fogging of the wind tunnel windows and instrument optics.

According to the assumption that all droplets are accelerated with the airflow in the long wind tunnel nozzle, the downstream position of the measurement volume in the test section should neither significantly affect the droplet diameter nor the droplet velocity or LWC. Depending on the mechanically required window configuration of the test section for every measurement setup, the downstream coordinate of the probe volume differed slightly. The measurement position of the PDI (or the RCT) and the shadowgraphy (or the FCDP) varied by a maximum of 220 mm (see Fig. 7) in downstream position.

To determine the desired number of droplets for a test point, one exemplary test point was measured over 15 minutes with the PDI system at constant test conditions. In a typical droplet size distribution in a spray in the wind tunnel, large droplets occur by orders of magnitude less frequent than small droplets (Rudoff et al., 1993; McDonell and Samuelsen, 1996). Therefore, the choice of the number of droplets per test point is essential for a representative and comparable determination of the MVD. Fig. 6 (left) shows the dependence of the MVD on the number of droplets taken into account. Since the MVD is sensitive to large droplets, its stability is a good hint for a representative measurement point. Taking into account more than 10000 droplets for the test point results in less than 5% deviation from the mean value over 280000 droplets. This minimum number of droplets was set as a target value for all experiments.

3 Measurement Techniques to determine PSD and LWC

Fig. 7 shows an overview of the different measurement setups in the BIWT. The following sections present the measurement instruments, their parametrization, as well as their inherent advantages and shortcomings. At the end of each section an estimation of the overall combined repeatability of the wind tunnel conditions and the precision of the treated measurement setup, based on repeated measurements is presented. The mean coefficients of variations obtained from several repetition tests are summarized in Table 4. When using optical methods, particular attention must be paid to the correct description and interpretation of the sample area, the cross-sectional area perpendicular to the flow velocity where droplets are detected. The sample area is defined by the optical and electronic configuration of the instrument (Widmann et al., 2001).

3.1 Phase Doppler Interferometry

The Phase Doppler Interferometry (PDI) is a single-particle counter, single point, real-time, and non-intrusive measurement technique and an extension of the Laser Doppler Anemometry (LDA), initially described in 1972 by Farmer (Farmer, 1972). Since the early 1980s, i.a. Bachalo has further advanced the principle into the PDI (Bachalo and Houser, 1984). The basic principle of LDA and PDI is based on the detection of the characteristic refraction signal of a spherical particle passing through an interference fringe pattern created by two coherent intersecting laser beams. The velocity of the particle (LDA) can be determined via the Doppler difference frequency of the scattered light signal. The spatial phase shift between the different detectors contains the size information of the particle (Durst and Zaré, 1975; Bachalo and Houser, 1984; Cossali and Hardalupas, 1992). The droplet diameter is estimated from the linear relationship of the phase difference with the diameter, a remarkable advantage over other optical probes that are based on intensity and diameter relationship which is sensitive to light attenuation and contaminated optics. In the PDI system, the receiver lens is additionally spatially partitioned into several segments. The PDI theoretically only needs an initial factory calibration because the parameters

responsible for the measurement results, like the laser wavelength, beam intersection angle, transmitter and receiver focal lengths, do not change within the lifetime of the system. Thus, PDI evolved as a common well characterized technique to measure spherical droplets in technical sprays, see Kapulla et al. (2007) and Jackson and Samuelsen (1987).

The PDI system used in this investigation is the 2D modular PDI from Artium Technologies Inc. It consists of an optical transmitter (diode-pumped solid-state laser), an optical receiver, Fourier-transform-based advanced signal analyzer (signal processors), a data management computer, and the AIMS system software. The PDI Transmitter has been used within two different setups: with a transmitter focal length of 350 mm in 2017 and 500 mm in 2019. The details of the used PDI system are summarized in Table 1.

Several early investigations of the PDI system have shown the effect of the photomultiplier tube (PMT) gain on the measurements (Bachalo et al., 1988; McDonell and Samuelsen, 1996). Thus, the PMT voltages were chosen carefully with regard to the expected diameter distribution and volume flux in the range of 300 to 390 Volts. The investigation of the sensitivity of the PDI setup to user-controlled settings of McDonell and Samuelsen (1990) showed variations in the MVD of 5%. The signal processor was therefore operated with the settings chosen by the manufacturer's automatic setup for the tests discussed here, to not add an additional source of variation in the results.

In the evaluation of the PDI results for size distribution and LWC, the probe volume correction (PVC) described inter alia in Zhu et al. (1993) was considered for all measurements. This correction is based on the assumption that smaller particles passing a Gaussian-shaped probe volume have only a smaller area where they can be detected because of their lower scattering intensity (scattering light can be taken as being proportional to the square of the droplet diameter (McDonell and Samuelsen, 1996)). Small particles need to pass the maximum intensity in the center of the probe volume to produce scattering signals high enough to be detectable. Larger droplets can still be detected when they pass at the edge of the Gaussian-shaped probe volume. Using the transit time method (Zhu, 1993), the real probe volume for every size class is measured independently and used for correction of the size distribution afterwards.

The calculation of the LWC from the PDI measurements is based on the corrected volume mean diameter D_{30}^{cor} and the corrected droplet number concentration N_d^{cor}, with the following formula (Widmann et al., 2001):

$$LWC = \frac{\pi}{6}\rho(D_{30}^{cor})^3\, N_d^{cor} \tag{4}$$

The corrected volume mean diameter of the size distribution D_{30}^{cor} is calculated with the probe volume corrected counts c_i^{cor} per size bin i.

$$D_{30}^{cor} = \sqrt[3]{\frac{\sum_{i=1}^{n} c_i^{cor} d_i^3}{\sum_{i=1}^{n} c_i^{cor}}} \tag{5}$$

$$c_i^{cor} = c_i\left(\frac{PV_{max}}{PV_i}\right)\left(\frac{D(d_i)_{max}}{D(d_{max})_{max}}\right) \tag{6}$$

Where d_i is the diameter of the i^{th} droplet size class and $D(d_{max})_{max}$ is the effective diameter where the light intensity is sufficient for the largest droplet to be detected. c_i is the uncorrected count in size class i. The probe volume corrected counts c_i^{cor} are related to the effective probe volume per size class PV_i, determined by the afore mentioned transit time method PV_{max} is the effective probe volume of the largest size class. For the calculation of the corrected droplet number concentration N_d^{cor}, the ratio of the total particle transit time $t_{tran(i,j)}$ and the total

sample time t_{Tot} is divided by the probe volume PV_i for each particle size class. The index i corresponds to size class and the index j corresponds to the droplet occurrence-

$$N_d^{cor} = \frac{1}{t_{Tot}} \sum_i \frac{\sum_j t_{tran(i,j)}}{PV_i} \quad (7)$$

The PVC has the greatest effect on the smallest size classes. Their influence on the LWC, on the other hand, is very small as it is dominated by the presence of large droplets. In addition to the PVC, an intensity validation scheme, described by Bachalo (2000), was used. This procedure supplements the PDI principle with a validity check, in which the agreement between signal intensity and droplet diameter calculated from the burst distance is checked. Overall, the approach to determine the LWC from the droplet size distribution increases the measurement uncertainties compared to direct LWC measurement methods (Lance et al., 2010), which has been shown e.g. by McDonell et al. (1994) and Widmann et al. (2001). McDonell et al. (1994) find variations in droplet concentration of up to 50%. Widmann et al. (2001) investigated the accuracy of LWC measurements from the PDI in an application with only low data rates and find a mean absolute value of the relative error of up to 26%. From these measurements it can be concluded that the droplet concentration is generally very sensitive to instrument operation and chosen settings. Because of the high number of influencing parameters, it is not surprising to see large variations in the results of re-runs (McDonell et al., 1994; Tropea, 2011). According to Bachalo et al. (1988) and Zhu et al. (1993), the calculation of the correct probe area is the primary source of error in the calculation of the volume flux.

The overall combined repeatability of the wind tunnel conditions and the precision of the PDI setup resulted over all tests with varied instrument settings and identical spray parameters in a mean coefficient of variation of the MVD of σ = 5%. DV0.1 and DV0.9 behave in a similar way, with an average coefficient of variation of σ = 7%. In the context of the measurements found in the literature mentioned above, the coefficient of variation determined here indicates an adequate design of the PDI system and the correct choice of system parameters. However, the average of the coefficient of variation over all repeatability measurements in DV0.99 is slightly greater (σ = 14%). The larger variation in DV0.99 is quite plausible since the very small proportion of large droplets can be detected statistically less frequently (see Fig. 8) but has a large impact on DV0.99 (McDonell et al., 1994). For this reason, their detection is affected by larger fluctuations even in measurements with a high number of total measured droplets. The LWC results show considerably more variability. The measured average coefficient of variation of about σ = 20% is four times greater than the variations in the MVD measurements but rather small if compared to McDonell et al. (1994), Widmann et al. (2001) and Tropea (2011). According to Equation 4 the LWC calculation of the PDI is proportional to the droplet number concentration N_d and to the third power of the corrected volume mean diameter D_{30}. The present coefficients of variation of the representative droplet diameters thus can lead directly to 15-21% variation in the LWC. Adding the uncertainty of the droplet number concentration the average coefficient of variation of 20% is coherent and comparatively small.

3.2 Fast Cloud Droplet Probe

The Fast Cloud Droplet Probe (FCDP) manufactured by SPEC Inc. is a single particle counter, which quantifies intensities of forward scattered light by particles passing through a laser beam to derive the particle's size and collate an overall number concentration. Forward scattering probes are generally used to detect microphysical

properties of liquid clouds from research aircraft (Lawson et al., 2017; Woods et al., 2018, McFarquhar, et al. 2017).

The particle size is determined via the correlation between the scattering cross-section under the assumption of Mie-theory and the signal voltage measured at the signal detector. A qualifying detector confines a focal area along the laser beam. This Sampling Area (SA) together with the incident true airspeed in transit time direction yields the sample volume (SV). A calibration of the SA size was performed by means of a beam mapping using a droplet generator according to Lance et al. (2010) or Faber et al. (2018). Detected particles are resolved into 21 size bins ranging from 1.5 µm up to 50 µm including one over-size bin, which was removed from further analyses. Bin widths range from 1.5µm, in the two lowest bins, up to 4µm for larger bin sizes. Some of the spray properties that can be derived from the measurements are the droplet number concentration N_d, MWD and LWC. The operation principle of the instrument, as well as general sources of uncertainties for this class of instruments are described in detail by Lance et al. (2010), Baumgardner et al. (2017), Lawson et al. (2017), Woods et al. (2018) and Faber et al. (2018).

Lance et al. (2010) report a particle sizing accuracy of a recalibrated and modified CDP of at least 10% (mainly due to the coarse size resolution of the size bins), which is also found in Faber et al. (2018). Although the referenced probes both lack the FCDP's novel optics and electronics, sizing accuracies might be of the same order of magnitude. However, Baumgardner et al. (2017) also report a propagated sizing uncertainty for single-particle scattering probes in general of 10% to 50%, where the advanced correction methods of the FCDP as a probe of the latest generation allocate this instrument at the lower side. The FCDP used in this study has novel fast electronics, which partially minimizes coincidence effects by calculating coincidence correction functions based on transit time information and other data stored with each individual particle. Further reductions in propagated uncertainty in droplet number concentration can thus be achieved under application of filtering techniques, such as transit time and inter particle arrival time filter methods of each individual droplet during post processing. Baumgardner et al. (2017) present a propagated droplet number concentration uncertainty between 10%-30% for the entire ensemble of forward scattering probes, where the FCDP again might be classified among the lower end. Unlike the PDI system used here, the FCDP was installed inside the test section of the wind tunnel with the sample volume placed in the undisturbed particle-laden flow at the center of the test section. Table 2 gives an overview of the main characteristics of the probe. For processing of N_d, the true airspeed (TAS) of the wind tunnel was also assumed as droplet velocity. The realization of high droplet number concentrations during our wind tunnel study and hence the increased probability of coincidence errors urges the use of a high DoF criterion, which is the ratio of qualifier to signal voltage of a detected droplet, in order to constrict the effective sample area and to limit coincidence effects. The SPEC manual recommends high DoF ratios for accurate particle sizing (FCDP SN6, SPEC 4/28/2017).

The calibration report also specifies a DoF ratio of 0.9 as the peak value for this specific probe. Initial variations of the DoF criterion support this recommendation.

An additional filtering method to further reduce coincident particles is provided by SPEC within a Matlab software module with which the theoretical full peak transit time of a droplet (TT) through a gaussian beam profile, depending on the droplet size and TAS, can be fitted to the measured TT versus size distribution using two fit parameter C1 and C3. Qualified scatter events outside the acceptance range of 25% beyond this theoretical TT to

size curve are regarded as coincident and are such discarded (SPECinc. C1C3_V4 manual, SPEC inc. Data Processing Manual 2012).

High particle number concentrations as in some conditions produced by the wind tunnel facility can be encountered in the atmosphere in polluted low clouds (Flammant et al., 2018; Taylor et al., 2019), polluted convection (e.g. Braga et al., 2017b; Ceccini et al., 2017) or in young contrails (e.g. Voigt et al., 2011; Kaufmann et al., 2014; Kleine et al., 2018).

In total, more than 80 different spray conditions have been measured each for about 120 s.

The repeatability of the wind tunnel conditions together with the precision of the measurement setup has been investigated for the FCDP, similarly to the PDI-setup. On average, a coefficient of variation of σ = 7% in MVD was found for all repetition measurements. Similar values were found for DV0.1 and DV0.9. Due to the large width of the size intervals (bins) of the FCDP for large particles, the determination of DV0.99 on the basis of the FCDP data was not further evaluated. Taking into account the accuracies of the FCDP for monodispersed single droplets, as mentioned above, the here found coefficients of variation of the representative droplet diameters indicate a good repeatability of the new spray system of the BIWT. Like the PDI results, the LWC calculations from the FCDP also show a significantly higher coefficient of variation (σ= 17%), inherent in the method of deriving the LWC from measurements of the particle's size, see Baumgardner (1983) and Tropea (2011).

3.3 Direct Imaging: Shadowgraphy

The idea of the shadowgraphy technique is to capture a high-resolution shadow image of a particle. In our study, a Litron Nano PIV–T double-pulsed laser is used as a light source. Its coherent light of 532 nm wavelength is diffused through a fluorescent plate, which illuminates the particles passing the system between the light source and camera. The spherical droplets are deflecting the incoming light wave, resulting in a particle shadow that is perceived from the observing camera. To obtain a high resolution for the droplet shadow images, 180 mm Tamron objective and magnification lenses (tele convertor 1,4X) were mounted in front of a PCO.4000 camera. The double-pulsed laser and the double-frame capability of the camera allow for the recording of short-time-separated pictures. This enables the droplet velocity computation by tracking the displacement of particles between two frames. The laser and camera are synchronized with an external programmable timing unit. Since the image acquisition rate of the camera is limited to approximately 2 frames per second, a long measurement time is required for a statistically robust result. For the correct interpretation of the measurement images, a prior calibration is necessary. The magnification factor of the optical array is determined by placing a transparent plate with a patterned array of dots (diameters from 10 µm to 200 µm) at the focal plane. Furthermore, a depth-of-field calibration is performed using the methodology of Kim and Kim (1994). The range in which droplets can be detected and correctly sized is limited by the image area of the camera chip, the depth-of-field of the optical system and the available light intensity. Finally, the shadow pictures are post-processed with an image analysis software (DaVis from LaVision), which determines the diameters of the shadow images in the field of view.

The image processing is performed on an inverted intensity image i.e. on the resultant of the shadow image subtracted from the background reference image (without particles). The subsequent particle detection is made relative to the difference between maximum and minimum of the inverted image, the noise can be eliminated with

a careful selection of minimum area and maximum area, eccentricity and other thresholds. The detailed post-treatment of shadow images has been described by Kapulla et al. (2007) and Kapulla et al. (2006).

The evaluation of the shadowgraphy pictures is rather focused on the size distribution and not on the LWC because of high uncertainties in the probe volume and consequently the droplet number concentration. The hardware settings used in the experiment conducted here are listed in Table 3. Because of the long measurement time for every test point (10 - 20 min), only 35 measurements in total were conducted. Among these 35 measuring points, there are many 2 to 3 times repeated measurements and measuring points with varied tunnel velocity but the same spray settings, leading to almost identical droplet size distributions in the evaluation (see test matrix in the supplementary material).

The combined influence of the precision of the shadowgraphy setup and the wind tunnel repeatability leads to an average variation of σ = 8% for the MVD, which is within the same order of magnitude compared to the afore-mentioned methods. According to Lefebvre and McDonell (2017), the imaging system developed by the Parker-Hannifin Corporation has a repeatability of 6% in the Sauter mean diameter range from 80 µm to 200 µm. Considering the significantly smaller droplets sizes here, the slightly higher coefficient of variation is plausible, as small droplets represent the more challenging task for direct imaging systems. Thus, the here measured variations indicate a well-chosen measurement setup and data post processing for the shadowgraphy technique.

3.4 Rotating Cylinder Technique

According to the SAE International Standard ARP5905 (Calibration and Acceptance of Icing Wind Tunnels), a rotating cylinder based on Stallabrass (1978) was designed and constructed for the BIWT. The rotation of the cylinder ensures a uniform ice build-up around the circular cross-section that provides aerodynamic consistency while accreting ice. If the speed of droplets, cylinder geometry, ice density, and collection efficiency (known droplet diameter) are known, the LWC can be calculated by the following formula:

$$LWC = \frac{\pi \cdot \rho_e}{\alpha_1 \cdot u_\infty \cdot t} \cdot \left[\left(\frac{m_e}{\pi \cdot \rho_e \cdot l_c} + r_c^2 \right)^{0,5} - r_c \right], \quad (8)$$

where ρ_e (assumed to be 880 kg m^{-3}) stands for the ice density, m_e for the final accreted ice mass, t for the icing time (selected with regard to the maximum allowed ice accumulation), α_1 for the collection efficiency, and l_c and r_c for the length and the radius of the original cylinder, respectively. The calculation of the collection efficiency is based on the assumption of a monodisperse droplet distribution with the MVD as the diameter for all droplets.

In this measurement method, several assumptions that lead to uncertainties in the LWC results are made. These are based on the SAE ARP5905 uncertainties in bulk density of ice, the simplification of the droplet size distribution to one representative diameter (MVD) and the assumption of a fixed cylinder diameter in the calculation of collection efficiency.

With the density of accreted ice depending on several parameters (temperature, droplet velocity, etc. (Macklin, 1962; Jones, 1990)), a 12.5% error in the assumed bulk density of ice leads to 3% error in LWC, according to Stallabrass (1978). King (1985) reiterates the accuracy of the rotating cylinder measurements under 10%. The simplification to regard the entire droplet cloud as a monodisperse spray with only droplets of the diameter of the MVD enters the calculation of the collection efficiency. Early investigations have shown that, for example, the assumption of a monodisperse droplet size distribution instead of a Langmuir D distribution of the droplet size leads to an overestimation of the collection efficiency of 3.5% at 25 m s^{-1} and MVD = 20 µm (Langmuir and

Blodgett, 1946). According to SAE ARP5905, the average diameter between non-iced and maximum iced cylinders for the calculation of the collection efficiency leads to an error of 1-2% in collection efficiency.
Two rotating cylinders were used for this testing with 2.5 mm (according to ARP5950) and 5 mm (for comparison) in diameter. The cylinders were rotated at 60 rpm. At the beginning of every run, the cylinder was shielded until the conditions had stabilized (approximately 15 s). All tests were performed at temperatures of - 18 °C or below to create rime ice, which is an essential requirement for this method (Ludlam, 1951). Differing from the previously mentioned systems, the RCT is an integrating and intrusive system. In this application, the MVD was taken from the PDI measurements and the LWC was measured by the RCT. In total, nearly 100 test points were done with 38 different spray settings.
The performed repeatability tests with the RCT lead to a coefficient of variation of $\sigma < 10\%$. Overall, SAE ARP5905 indicates because of the mentioned sources of errors a method accuracy of > 90%, which can be verified by the repetition measurements carried out in this study.

3.5 LWC based on Water Flow Rate and Wind Tunnel Speed

The LWC in the icing wind tunnel can be determined from the total injected water mass flow and the circulating air volume flow (Biter (1987)). There are two prerequisites for the application of this procedure:
1) there is no recirculating water;
2) there is a known moist air volume flow (depending on flow velocity and droplet size).
The first assumption is true for an air temperature below 0 °C. In these conditions, the droplets will supercool and freeze out by hitting a surface of the wind tunnel, e.g. turning vanes of the first or second corner, collecting grid, fan or heat exchanger. To determine the moistened air volume flow in the wind tunnel, several icing tests on a grid were performed. The area over which the droplets spread depends on the wind tunnel speed and the droplet size or the air pressure used at the spray nozzles for droplet generation. Several tests were performed to measure the 2D-iced area in the test section and to estimate the LWC in the borders close to the wind tunnel walls. On the basis of these assumptions, the LWC can be calculated with the following formula:

$$LWC = \frac{\dot{m}_{Water}}{\dot{V}_{Air}} = \frac{\dot{m}_{Water}}{\alpha \cdot A_{testsection} \cdot u_{\infty}}, \quad (9)$$

where $\dot{m}_{Water}$ is the injected water mass flow, α is the percentage of the moistened cross-sectional area, $A_{testsection}$ the cross-sectional area, and u_{∞} the tunnel velocity. These numbers are available for all measurements and take also into account the clogging of nozzles during the experiment. Thereby, this method offers a good reference for LWC comparison.

The overall accuracy of the mass-flow-based-calculation of the LWC is primarily limited by the accuracy in the measurement of the water mass flow and the uncertainty in the determination of the moistened cross-sectional area. The water volume flow is measured with one thermal volumetric flow meter per row of six atomizers. Due to the very low total water volume flow through every thermal volumetric flow meter (down to less than 10 ml min^{-1} per row) and the pulsation of the nozzles, the uncertainty of the volume flow measurement is

approximately 20%. The mean coefficient of variation of repeated test cases for the calculated LWC over the water mass flow and the moistened air volume is σ = 7%.

4 Experimental Results and Discussion

The results of the intercomparison of the different measurement techniques are presented in this section. Tropea (2011) identifies three main sources of error in the measurement of size distributions with optical techniques, liquid fluxes, and droplet number concentration, which are inherent in all optical measurements conducted here: errors in droplet sizing, errors in counting (missed particles, coincidence) and errors in the sampling area (or volume) estimation.

The measurement uncertainties in droplet number concentration and sizing result in greater uncertainties for higher-order products such as LWC calculated from the observed cloud droplet size distribution (Lance et al. 2010).

4.1 Comparison of MVD measurements from the different instruments

The particle size distribution obtained from the different measurement techniques is studied for two spray settings, resulting in a MVD of 14.5 µm and a larger MVD of 33.8 µm, see Fig. 9. The plot shows almost a similar trend for all the measurements despite their different acquisition rates, suggesting the acquisition time is sufficiently large for each of the methods. For the MVD 14.5 µm series, all measurement techniques show a mutual agreement in the distribution of normalized droplet counts. FCDP observations show slightly higher relative counts between 7 and 9 µm. Mode maximum of the PDI_{FCDP} normalized droplet curve is found to be around 5µm and shifted towards smaller sizes, compared to the other techniques, but catches up with the curves for FCDP and shadowgraphy beyond 11 µm and 15 µm respectively. Sizing of smaller droplets with the FCDP are subject to errors due to Mie ambiguity. The droplet sizing from PDI is obtained by using linear relations between the phase shift and size derived for a predominant reflection or refraction mode and applying principles of geometrical optics (Ofner 2001). Below 5 µm, the validity of the geometric optics tends to cease and the diffraction becomes significant leading to erroneous measurements (Chuang 2008). Bachalo and Sankar (1996) reported the uncertainties resulting from these oscillations to be under ±0.5 µm. Due to the resolution limit and the depth-of-field problem of the shadowgraphy technique, its PSD is shifted towards higher droplet sizes, ultimately distorting its cumulative liquid water content plot for larger droplet diameters. For the MVD 33.8 µm series, similar observations can be made. Noteworthily, the FCDP with its sizing limit of 50 µm does not allow to evaluate the upper end of the PSD, where shadowgraphy still enables optical accessibility. The representation of larger droplets is the lowest of the presented measurement techniques, in terms of droplet counts, whereas an abundance of observed droplets is visible between 7 and 9 µm.

A further analysis of the measurement techniques is based on the MVD as a scalar representation of the PSD, using again the PDI as a reference instrument, see Fig. 10. To compare FCDP and PDI results, the range of the PDI data evaluated for the intercomparison was limited to a maximum droplet diameter of 50 µm in a post-processing step to match the upper particle size limit of the FCDP.

The linear best fit ($MVD_{FCDP}=0.91 \cdot MVD_{PDI}$) through the data points has a coefficient of determination of $R^2=0.9853$. The mean absolute value of the relative difference between the FCDP and the PDI measurements is

$|E_{FCDP - PDI}|$ = 7.7% ± 3.9%. When comparing the relative deviations of the two instruments, for PSDs with MVDs < 20 µm the agreement between PDI and FCDP is nearly 100% and for distributions with MVDs > 20 µm the FCDP measures on average 9% lower MVDs compared to the PDI (see Fig. 11 left). Declining counts towards larger particle sizes (> 30 µm) may cause or contribute to the measured deviation of the FCDP with respect to the PDI for large droplets.

Confining the SA by application of a strict DoF criterion as a countermeasure in order to constrain coincidence in these high droplet number conditions might reduce the sample statistics for larger droplets and thus leading to an under representation of larger droplets contributing to the MVD in respective test points. Thornberry et al. (2016) also report an under counting of larger particles when comparing the overlap region between a FCDP and a 2D-S probe.

Measured droplet number concentrations up to 2000 cm^{-3} from FCDP compared to PDI follow a linear distribution with a coefficient of determination of R^2=0.9299 and a tendency of observed higher N_d. The mean absolute value of the relative error is 34% ±29% (Fig. 12). Data points beyond 2000 cm^{-3} are scarce and deviate clearly from the afore mentioned trend for smaller N_d. This saturation effect, visible in the FCDP droplet number concentrations, might indicate the onset region of remaining coincident effects on particle counts to be located between 1500 cm^{-3} and 2000cm^{-3} under consideration of the applied settings.

An additional source of error might be introduced via the external geometry of the probe and modified droplet trajectories which might alter the measured cloud particle size distribution (Weigel et al. 2016); although this is accounted for to a certain extent by the aerodynamic shape of the FCDP, which differs from those in previous studies analyzed blunt geometry of classical PMS probes. Uncertainties due to aerodynamic effects still have to be considered while comparing measurements from the FCDP with non- intrusive techniques in the comparatively small test section of BIWT.

An evaluation of the implemented shattering filter in the post processing routines provided by SPEC, based on particle inter arrival time attributes shattering a negligible role. This may be due to the absence of very large droplets and ice particles, as well as the use of anti-shattering tips (Korolev et al., 2013, McFarquhar et al., 2007). Ice accretion on the non-heated parts of the probe might additionally alter the local two-phase flow in the upstream direction (see Fig. 7).

The generally good agreement in MVD between FCDP and PDI in the size range of 8 to 35µm with up to 14% deviation is well within the range of other instruments intercomparisons (Faber et al., 2018; Braga et al., 2017).

To ensure mutual size ranges between the PDI and the shadowgraphy system the minimum diameter of the PDI results was corrected to 10 µm in post-processing. The results of the shadowgraphy measurements are depicted in Fig. 10 as circles. Larger variations were detected by shadowgraphy for particle sizes larger than 35 µm.

The linear best fit ($MVD_{Shadowgraphy}$=0.97·MVD_{PDI}) through the data points with a MVD < 35 µm has a coefficient of determination of R^2=0.7985 and is therefore smaller than the one from the FCDP data. The mean absolute value of the relative difference between the shadowgraphy and the PDI measurements is $|E_{Shadowgraphy - PDI}|$ = 9.9% ± 6.3%. The eight outlier with higher MVD_{PDI} have not been taken into account for the best fit curve. An explanation for these measuring points with significantly smaller MVD again can be found in the typical drop size distribution: sample statistics suffer from a declining proportion of large droplets. (see Fig. 8). Rudoff et al. (1993) showed also in NASA's Glenn Research Center's Icing Research Tunnel (IRT) that the droplet distribution can have a long tail towards large droplets, which can only be detected reliably with

exceptionally long measurement durations. With the shadowgraphy setup used here, only very low data rates could be measured. As a result, often only 3000-6000 droplets per spray condition were measured despite long test times (> 15 min) for one condition only. The Droplet size distribution, however, can only be slightly corrected for large droplets, if at all, by application of a border correction. With the DoF and border correction, this leads to an average of more than 20000 droplets per distribution. The overall agreement between shadowgraphy and PDI results matches previous measurements, e.g. Kapulla et al. (2007) and Rydblom et al. (2019).

4.2 Comparison of LWC measurements from the different instruments

Fig. 13 shows the measurement results of the PDI, the FCDP, and the RCT compared to the LWC calculated from the injected water mass flow. Generally bulk phase instruments such as the rotating cylinder or a hotwire are used for the determination of the LWC. As expected, the comparison shows a significantly greater degree of variation compared to the droplet size results, which is discussed in more detail in the following.

The mean absolute value of the relative difference between the PDI results and the LWC calculation based on the water flow rate is $|E_{PDI\ -\ WFR}| = 24\% \pm 28\%$. Despite the large absolute value of relative difference, the mean best fit line ($LWC_{PDI} = 0.98 \cdot LWC_{WFR}$ with coefficient of determination of $R^2=0.8503$) fits well to the results of the water mass flow method. From over 70 data points with $LWC_{WFR} < 0.5$ g m^{-3}, 84% from the PDI results fall within a range of ± 0.1 g m^{-3} around the LWC_{WFR} (71% of $LWC_{WFR} < 0.3$ g m^{-3} in the range ± 0.05 g m^{-3}). Chuang et al. (2008) performed an intercomparison of the airborne PDI to a Gerber Scientific Inc. PVM-100A (a probe based on forward light scattering (Gerber et al., 1994)) and obtained a good consistency for LWC of up to 0.3 g m^{-3} with an accuracy of ± 0.05 g m^{-3} containing 85% of data points, which, despite the different velocities, is in good agreement with the results obtained here. Of the more than 100 remaining measurement results of the PDI with an LWC > 0.5 g m^{-3}, only 57% lie within a range of ± 20% around the LWC calculated from the water mass flow. Cober et al. (2012) compare the integrated LWC from in situ measurements in supercooled large droplet conditions from FSSP and 2D-C and 2D-P to the results of the Nevzorov probe. A slightly higher LWC result from the integrating systems was found compared to the Nevzorov probe. From the measurements of Cober et al. (2012) with LWC > 0.1 g m^{-3}, 85% of the measurement points agree within ± 43% with that of the Nevzorov results. In our experiments, 90% of all PDI results with an LWC > 0.1 g m^{-3} agree within less than ± 43% deviation to the water flow rate. Therefore, our results, which partly also contain droplets > 100 µm, are comparable to the results of the flight tests of Cober et al. (2012).

For a detailed analysis of the LWC results of the PDI, Fig. 14 shows the ratio of LWC_{PDI} to LWC_{WFR} over the MVD measured by the PDI and over the air velocity in the wind tunnel. Plotting the LWC over the MVD indicates no clear tendency. Plotting the LWC ratio against the wind tunnel velocity shows that at low velocities the PDI results are above the LWC calculated over the mass flow and with increasing velocities the LWC_{PDI} tends to become lower than the reference values. A similar result was obtained by Rudoff et al. (1993) for the IRT. To see whether this dependency can be attributed more to the wind tunnel and the water mass flow methodology or the PDI, the other measurement techniques are first examined in detail.

If also assuming an uncertainty of ± 20% for the PDI results, more than 85% of the LWC measurement data overlap between the PDI and water mass flow. The comparison of the measurement results supports the already mentioned greater uncertainty in the LWC measurements.

The results of the FCDP show a larger variation with respect to the reference. The linear best fit $LWC_{FCDP} = 1.12 \cdot LWC_{WFR}$ has a coefficient of determination of $R^2=0.3276$. Overall, there is a systematic high bias of the LWC derived from the FCDP compared to the PDI, despite eventually smaller particle sizes detected by the FCDP. This can only be explained by higher particle number concentrations measured by the FCDP compared to the PDI, as can be seen in Fig. 12. An overestimation of the LWC by the use of scattering spectrometers has been found previously in comparative experiments (Rydblom et al., 2019; Faber et al., 2018; Ide, 1999). For the FSSP forward scattering probe, Baumgardner (1983) found 20-200% higher LWC values than measured by hot-wire probes. In the measurements by Ide (1999), the LWC calculated from the droplet diameter distributions overestimated the LWC for MVDs up to 50 µm by 50% and even up to 100% and 150% for higher MVDs. Faber et al. (2018) have suggested the velocity difference between his laboratory measurements and aircraft measurements, for which the CDP is originally designed, as a possible reason for the large overestimation of LWC. This could also be a possible explanation for the results obtained here. To examine the results in detail, Fig. 15 shows the ratio of LWC_{FCDP} to LWC_{WFR} versus MVD_{FCDP} and versus $N_{d\,FCDP}$.

Unlike the PDI, a correlation between the FCDP data for LWC and droplet size seems to be obvious. Measurements with an MVD > 27 µm are the only ones leading to an underestimated LWC. These measurement points also correspond to the data points with low data rates and low particle concentrations (see the right section of Fig. 15). Due to the limited size range of the FCDP and the broad width of the size bins, the underestimation of the LWC can be caused by some of the droplets present in the flow but not visible for the FCDP. At high N_d and small droplet diameters, the FCDP significantly overestimates the LWC. The dependence of LWC on droplet concentration was also observed by Lance et al. (2010) in observations during the ARCPAC campaign. Also a larger contribution of small droplets to an LWC overestimation bias is confirmed from simulations (Lance et al. (2010)). Higher droplet number concentration exhibits higher coincidence effects and lead to overestimated particle sizes. However, Fig. 10 clearly shows an agreement of 7% within the probes and eventually a low bias of the MVD detected with the FCDP.

The results of the RCT are illustrated by blue circles in Fig. 13. The mean absolute value of the relative difference between the rotating cylinder and the LWC calculation based on the water flow rate is $|E_{rotCyl\ -\ WFR}| = 22.9\% \pm 21.3\%$ and is therefore the smallest among the presented LWC measurements. The linear best fit ($LWC_{rotCyl}=0.98 \cdot LWC_{WFR}$) over the data points has a coefficient of determination of $R^2=0.9066$. Taking into account an uncertainty of ± 10% in the measurement results of the rotating cylinder, 78% of the measurement points are within the range of the expected value regarding to water mass flow. Cober et al. (2001) compared the integrated LWC of the droplet sizing probes to the measurement results from the Rosemount icing (ice-accretion-based) detector, where 90% of the data fall within the 1:1 correlation ± 64%. The large scatter of these data is similar to the measurements described here, although the comparison technique is different.

Fig. 14 shows that both with increasing MVD and velocity the LWC tends to be slightly overestimated by the RCT. Ide (1999) found in his measurements a good agreement between the icing blade, the RCT, and two hot-wire-probes for small droplets (MVD < 40 µm). This outcome can be supported by the results presented in this study. When compared to the PDI, the RCT behaves in the exact opposite way: the LWC from the PDI measurements tend to decrease with increasing velocity, whereas the LWC from the RCT is increasing with velocity. This contrary behaviour of the two different measurement techniques calls rather not for a cause in the methodology of the water mass flow but causes in the individual measurement techniques.

5 Summary and Outlook

The BIWT has been further developed to produce liquid droplets in the size range of 1 to 150 µm at LWC ranges of 0.1 to 2.5 g m^{-3}. The droplets were accelerated to velocities between 10 and 40 m s^{-1} and supercooled to temperatures between 0 and -20 °C. Measurements with the PDI show that the icing wind tunnel exhibits a good repeatability of the MVD with a stability better than 3% and the LWC to be better than 7%, as derived by standard variation. These test conditions permit very high reliability and stability appropriate to intercompare various droplet measuring techniques.

A probe intercomparison study of droplet size (PDI, FCDP, and shadowgraphy) and LWC (PDI, FCDP, and RCT) measurement systems was performed. Generally, the MVD measured with the FCDP agreed within 15% to measurements with the PDI, which is in the range or better than previous tests in wind tunnels. The MVD of the shadowgraphy agreed up to 35 µm well to the PDI, beyond MVD 35 µm a higher discrepancy was observed. By comparing the droplet size measurement techniques, it was possible to identify some measurement system-dependent sources of uncertainties. For the FCDP, the high sensitivity of the transit time filter to velocity differences of the droplets or a respective low sensitivity to larger particle sizes (>35 µm) was hypothesized. Our results with the shadowgraphy setup also show the importance of the upper part of the droplet size distribution, where the occurrence of larger droplets declines. The fraction of large droplets has a huge impact on characteristic quantities such as the MVD and therefore requires a high number of sampled droplets per measurement point.

In addition, LWC measurements were compared to the LWC calculated from wind tunnel input parameters and the flow rate. Here, besides the rotating cylinder bulk phase instrument, the LWC was also derived from the PSD measured with the single particle probes, albeit with larger uncertainty. 57% (59%) of the LWC results measured with the RCT (PDI) agreed within 20% with the LWC determined based on the water mass flow. This is also a good overall agreement compared to existing tests. Several technology-dependent differences and error sources were identified for the LWC measurements. The PDI results showed a slight overestimation of the LWC with decreasing flow velocity. The RCT results showed very good agreement to the LWC results based on water mass flow, especially for small droplet sizes, concurring well with literature studies. The FCDP results differ significantly (factor of 0.5 to 3) from the water mass flow results.

Based on these new results on the performance of the BIWT for unimodal droplet distributions and related strength and shortcomings of instruments and measurement systems detecting PSDs and LWCs, future plans are to further enhance the capacity of the BIWT's spray system to generate bimodal droplet size distributions according to EASA CS 25 Appendix O. These distributions incorporate one collective of small droplets (around 11-14 µm) and a second collective of very large droplets (around 160-200 µm), while requiring a low LWC between 0.1 and 0.45 g m^{-3}. The reliable acquisition of both modes with the associated low number density of the large droplets > 100 µm poses new challenges for droplet measurement techniques. The detection range has to be extended and the trajectory of large droplets and their sedimentation velocity has to be considered in the wind tunnel design and probe layout in order to accurately provide and measure a large particle spectrum. Existing knowledge in ice crystal icing experiments (e.g. Bansmer et al., 2018) can support these developments.

The Supplement related to this article is available online at via doi:

Author contribution

Inken Knop designed and carried out most of the described experiments. The FCDP measurements were designed and carried out by Valerian Hahn, supported by Inken Knop. Stephan Bansmer and Christiane Voigt supported the post processing and evaluation of the experiments, mainly conducted by Inken Knop (and Valerian Hahn for the FCDP). Inken Knop prepared the manuscript with the contributions from all co-authors. The authors would like to thank Venkatesh Bora in supporting the review process of the paper.

Competing interests

The authors declare that they have no conflict of interest.

Acknowledgements. The presented work was conducted within the framework of the project Drífa -FKZ0325842A funded by the German Federal Ministry of Economic Affairs and Energy. Christiane Voigt and Valerian Hahn were funded by the European Union H2020 programme ICE GENESIS under contract number 824310 and by the DFG within SPP2115 PROM under contract number VO1504/5-1. The PDI measurements were strongly supported by Dr. Thomas Brämer and David Apel from LaVision GmbH, Göttingen, Germany. The authors further express their thanks to Biagio Esposito (CIRA) and Will Bachalo (Artium) for their help in interpreting the PDI results and Stephan Sattler (TU Braunschweig) and Oliver Esselmann (former TU Braunschweig) in conducting the experiments. Finally, the authors acknowledge the support of the Open Access Publication Funds of the Technische Universität Braunschweig.

References

AGARD NATO: Quality Assessment for Wind Tunnel Testing. AGARD-AR-304, 1994.

Anderson, D. N.: Manual of scaling Methods, NASA/CR -2004-212875, 2004.

ARP5905: Calibration and Acceptance of Icing Wind Tunnels. Available online at https://www.sae.org/standards/content/arp5905/, 2015, last access: 23 July 2019.

Bachalo, W. D.; Spray diagnostics for the twenty-first century. In *Atomization and Sprays* 10.3-5 (2000): 439-474.

Bachalo, W. D.; Houser, M. J.: Development of the phase/doppler spray analyzer for liquid drop size and velocity characterisations. AIAA-84-1199, https://arc.aiaa.org/doi/pdf/10.2514/6.1984-1199,1984.

Bachalo, W. D.; Houser, M. J.: Phase/Doppler Spray analyzer for simultaneous measurements of drop size and velocity distributions. In *Opt. Eng* 23 (5), 235583, https://doi.org/10.1117/12.7973341, 1984.

Bachalo, W. D.; Rudoff, R. C.; Brena de la Rosa, A.: Mass Flux Measurements of a High Number Density Spray System Using the Phase Doppler Particle Analyzer, AIAA 26th Aerospace Sciences Meeting, Reno, January 11-14, https://doi.org/10.2514/6.1988-236, 1988.

Bansmer, S. E.; Baumert, A.; Sattler, S.; Knop, I.; Leroy, D.; Schwarzenboeck, A. et al.: Design, construction and commissioning of the Braunschweig Icing Wind Tunnel. In Atmos. Meas. Tech. 11 (6), pp. 3221–3249. https://doi.org/10.5194/amt-11-3221-2018, 2018.

Bartlett, C. S.: Icing Scaling Considerations for Aircraft Engine Testing, AlAA 26th Aerospace Sciences Meeting, AIAA-88-0202, https://arc.aiaa.org/doi/pdf/10.2514/6.1988-202, 1988.

Battisti, L.: Wind turbines in cold climates. Icing impacts and mitigation systems, Green energy and technology, Springer International Publishing, Switzerland, 2015.

Baumgardner, D.; Abel, S. J.; Axisa, D.; Cotton, R.; Crosier, J.; Field, P. et al.: Cloud Ice Properties - In Situ Measurement Challenges. In Meteorological Monographs 58, p. 9.1. https://doi.org/10.1175/AMSMONOGRAPHS-D-16-0011.1, 2017.

Baumgardner, D.: An Analysis and Comparison of Five Water Droplet Measuring Instruments. In J. Climate Appl. Meteor. 22 (5), pp. 891–910, https://doi.org/10.1175/1520-0450(1983)022<0891:AAACOF>2.0.CO;2, 1983.

Biter, C. J., et al., 1987: The drop-size response of the CSIRO liquid water probe. J. Atmos. Oceanic Technol. 4, 359-367.

Bossard, J. A.; Peck, R. E.: Droplet size distribution effects in spray combustion, Symposium (International) on Combustion 26 (1), pp. 1671–1677. https://doi.org/10.1016/S0082-0784(96)80391-2, 1996.

Braga, R. C., Rosenfeld, D., Weigel, R., Jurkat, T., Andreae, M. O., Wendisch, M., Pöhlker, M. L., Klimach, T., Pöschl, U., Pöhlker, C., Voigt, C., Mahnke, C., Borrmann, S., Albrecht, R. I., Molleker, S., Vila, D. A., Machado, L. A. T., and Artaxo, P.: Comparing parameterized versus measured microphysical properties of tropical convective cloud bases during the ACRIDICON–CHUVA campaign, In *Atmos. Chem. Phys*., 17, 7365-7386, https://doi.org/10.5194/acp-17-7365-2017, 2017.

Braga, R. C., Rosenfeld, D., Weigel, R., Jurkat, T., Andreae, M. O., Wendisch, M., Pöschl, U., Voigt, C., Mahnke, C., Borrmann, S., Albrecht, R. I., Molleker, S., Vila, D. A., Machado, L. A. T., and Grulich, L.: Further evidence for CCN aerosol concentrations determining the height of warm rain and ice initiation in convective clouds over the Amazon basin, Atmos. Chem. Phys., 17, 14433-14456, https://doi.org/10.5194/acp-17-14433-2017, 2017b.

Brenguier, J.-L.; Bourrianne, T.; Coelho, A. A.; Isbert, J.; Peytavi, R.; Trevarin, D.; Weschler, P.: Improvements of Droplet Size Distribution Measurements with the Fast-FSSP (Forward Scattering Spectrometer Probe). In J. Atmos. Oceanic Technol. 15 (5), pp. 1077–1090. https://doi.org/10.1175/1520-0426(1998)015%3C1077:IODSDM%3E2.0.CO;2 1998.

Cecchini, M. A., Machado, L. A. T., Andreae, M. O., Martin, S. T., Albrecht, R. I., Artaxo, P., Barbosa, H. M. J., Borrmann, S., Fütterer, D., Jurkat, T., Mahnke, C., Minikin, A., Molleker, S., Pöhlker, M. L., Pöschl, U., Rosenfeld, D., Voigt, C., Wenzierl, B., and Wendisch, M.: Sensitivities of Amazonian clouds to aerosols and updraft speed, Atmos. Chem. Phys., 17, 10037-10050, https://doi.org/10.5194/acp-17-10037-2017, 2017.

Chuang, P. Y.; Saw, E. W.; Small, J. D.; Shaw, R. A.; Sipperley, C. M.; Payne, G. A.; Bachalo, W. D.: Airborne Phase Doppler Interferometry for Cloud Microphysical Measurements. In Aerosol Science and Technology 42 (8), pp. 685–703. https://doi.org/10.1080/02786820802232956, 2008.

Cober, S. G., G. A. Isaac, and J. W. Strapp, 2001: Characterizations of Aircraft Icing Environments that Include Supercooled Large Drops. J. Appl. Meteor., 40, 1984–2002, https://doi.org/10.1175/1520-0450(2001)040<1984:COAIET>2.0.CO;2., 2001.

Cober, S. G.; Isaac, G. A.: Characterization of Aircraft Icing Environments with Supercooled Large Drops for Application to Commercial Aircraft Certification. In J. Appl. Meteor. Climatol. 51 (2), pp. 265–284. https://doi.org/10.1175/JAMC-D-11-022.1, 2012.

Coleman, H. W., Steele, W. G.: Engineering application of experimental uncertainty analysis, AIAA Journal, 33(10), 1995.

Cossali, E.; Hardalupas, Y.: Comparison between laser diffraction and phase Doppler velocimeter techniques in high turbidity, small diameter sprays. In Experiments in Fluids 13 (6), pp. 414–422. https://doi.org/10.1007/BF00223249, 1992.

Dodge, L. G.: Comparison of performance of drop-sizing instruments. In Applied optics 26 (7), pp. 1328–1341. https://doi.org/10.1364/AO.26.001328, 1987.

EASA: Certification Specifications and Acceptable Means of Compliance for Large Aeroplanes. CS-25, revised 18. Available online at https://www.easa.europa.eu/sites/default/files/dfu/CS-25%20Amendment%2018_0.pdf, 2016, last access: 1 July 2019.

Federal Aviation Administration, 14 CFR 25, Airworthiness standards: Transport category airplanes. https://www.govinfo.gov/content/pkg/CFR-2011-title14-vol1/pdf/CFR-2011-title14-vol1-part25.pdf, last access: 10 September 2020.

Faber, S.; French, J. R.; Jackson, R.: Laboratory and in-flight evaluation of measurement uncertainties from a commercial Cloud Droplet Probe (CDP). In Atmos. Meas. Tech. 11 (6), pp. 3645–3659. https://doi.org/10.5194/amt-11-3645-2018, 2018.

Fansler, T. D.; Parrish, S. E.: Spray measurement technology: A review. In Meas. Sci. Technol. 26 (1), p. 12002. https://doi.org/10.1088/0957-0233/26/1/012002, 2015.

Farzaneh, M. (Ed.): Atmospheric Icing of Power Networks. Dordrecht: Springer, Netherlands, 2008.

Flamant, C., P. Knippertz, A.H. Fink, A. Akpo, B. Brooks, C.J. Chiu, H. Coe, S. Danuor, M. Evans, O. Jegede, N. Kalthoff, A. Konaré, C. Liousse, F. Lohou, C. Mari, H. Schlager, A. Schwarzenboeck, B. Adler, L. Amekudzi, J. Aryee, M. Ayoola, A.M. Batenburg, G. Bessardon, S. Borrmann, J. Brito, K. Bower, F. Burnet, V. Catoire, A. Colomb, C. Denjean, K. Fosu-Amankwah, P.G. Hill, J. Lee, M. Lothon, M. Maranan, J. Marsham, R. Meynadier, J. Ngamini, P. Rosenberg, D. Sauer, V. Smith, G. Stratmann, J.W. Taylor, C. Voigt, and V. Yoboué, 2018: The Dynamics–Aerosol–Chemistry–Cloud Interactions in West Africa Field Campaign: Overview and Research Highlights, Bull. Amer. Meteor. Soc., 99, 83–104, https://doi.org/10.1175/BAMS-D-16-0256.1, 2018.

Gerber, H.; Arends, B. G.; Ackerman, A. S.: New microphysics sensor for aircraft use. In Atmospheric Research 31 (4), pp. 235–252. https://doi.org/10.1016/0169-8095(94)90001-9, 1994.

Gurganus, C., and *P. Lawson*, Laboratory and Flight Tests of 2D Imaging Probes: Toward a Better Understanding of Instrument Performance and the Impact on Archived Data, 2018: J. Atmos. Ocean Technol., https://doi.org/10.1175/JTECH-D-17-0202.

Ide, R. F.: Comparison of Liquid Water Content Measurement Techniques in an Icing Wind Tunnel, NASA/TM - 1999-209643, 1999.

Ide, R.F., Oldenburg, J.R., Icing Cloud Calibration of the NASA Glenn Icing Research Tunnel, American Institute of Aeronautics and Astronauticsdoi: 10.2514/6.2001-234, 2001.

Jackson, T. A.; Samuelsen, G. S.: Droplet sizing interferometry: a comparison of the visibility and phase/Doppler techniques. In Applied optics 26 (11), pp. 2137–2143. https://doi.org/10.1364/AO.26.002137, 1987.

Jones, K. F.: The density of natural ice accretions related to nondimensional icing parameters. In Q.J Royal Met. Soc. 116 (492), pp. 477–496. https://doi.org/10.1002/qj.49711649212, 1990.

Kapulla, R. Trautmann, M.; Güntay, S.; Dehbi, A.; Suckow, D.: Comparison between phase-Doppler anemometry and shadowgraphy systems with respect to solid-particle size distribution measurements. Edited by D. Dopheide, H. Müller, V. Strunck, B. Ruck, A. Leder. GALA e.V. Deutsche Gesellschaft für Laser-Anemometrie. Braunschweig (Lasermethoden in der Strömungsmesstechnik, 13), 2006.

Kapulla, Ralf; Trautmann, Mathias; Hernandez Sanchez, Alicia; Calvo Zaragoza, Salvador; Hofstetter, Sarah; Häfeli, Christoph et al.: Droplet size distribution measurements using phase-Doppler anemometry and shadowgraphy: Quantitative comparison, GALA e.V. Deutsche Gesellschaft für Laser-Anemometrie. Rostock (Lasermethoden in der Strömungsmesstechnik, 15), 2007.

Kaufmann, S., C. Voigt, P. Jeßberger, T. Jurkat, H. Schlager, A. Schwarzenboeck, M. Klingebiel, and T. Thornberry: In situ measurements of ice saturation in young contrails, Geophys. Res. Lett., 41, https://doi.org/10.1002/2013GL058276, 2014.

Kim, K. S.; Kim, S.-S.: Drop Sizing and depth-of-field correction in TV imaging. In Atomiz Spr 4 (1), pp. 65–78. https://doi.org/10.1615/AtomizSpr.v4.i1.30, 1994.

King, W.D.; Dye, J. E.; Strapp, J. W.; Baumgardner, D.; Huffmann, D.: Icing wind tunnel tests on the CSIRO liquid water probe. J. Atmospheric and oceanic technology. Vol. 2, pp. 340-352. https://doi.org/10.1175/1520-0426(1985)002%3C0340:IWTTOT%3E2.0.CO;2 ,1985.

Kleine, J., C. Voigt, D. Sauer, H. Schlager, M. Scheibe, S. Kaufmann, T. Jurkat-Witschas, B. Kärcher, B. Anderson: In situ observations of ice particle losses in a young persistent contrail, Geophs. Res. Lett., https://doi.org/10.1029/2018GL079390, 2018.

Korolev, A., Emery, E., Creelma, K.: Modification and tests of particle probe tips to mitigate effects of ice shattering. J. Atmos. Oceanic Technol., 30, 690-708, 2013.

Kreeger, R. E.; Sankar, L.; Narducci, R.; Kunz, R.: Progress in Rotorcraft Icing Computational Tool Development. SAE Technical Paper 2015-01-2088, 2015.

Lance, S.; Brock, C. A.; Rogers, D.; Gordon, J. A.: Water droplet calibration of the Cloud Droplet Probe (CDP) and in-flight performance in liquid, ice and mixed-phase clouds during ARCPAC. In Atmos. Meas. Tech. 3 (6), pp. 1683–1706. https://doi.org/10.5194/amt-3-1683-2010, 2010.

Lance, S.: Coincidence errors in a cloud droplet probe (CDP) and a cloud and aerosol spectrometer (CAS), and the improved performance of a modified CDP, J. Atmos. Ocean. Technol., 29, 1532−1541, https://doi.org/10.1175/JTECH-D-11-0208.1, 2012.

Langmuir, I.; Blodgett, K.B.: The collected works of Irving Langmuir, Volume 10 - Atmospheric phenomena, chap. A Mathematical Investigation of Water Droplet Trajectories., 335-393, Pergamon press, 1961.

Lawson, R. P., *C. Gurganus*, *S. Woods*, and R. Bruintjes, Aircraft Observations of Cumulus Microphysics Ranging from the Tropics to Midlatitudes: Implications for "New" Secondary Ice Process: J. Atmos. Sci., 74, 2899-2920, 2017.

Lefebvre, A. H.; McDonell, V. G.: Atomization and sprays. Second Edition. Boca Raton, London, New York: CRC Press. 2017.

Linne, M.: Imaging in the optically dense regions of a spray: A review of developing techniques. In Progress in Energy and Combustion Science 39 (5), pp. 403–440. https://doi.org/10.1016/j.pecs.2013.06.001, 2013.

Liu, H.-F.; Gong, X.; Li, W.-F.; Wang, F.-C.; Yu, Z.-H. Prediction of droplet size distribution in sprays of prefilming air-blast atomizers. In Chemical Engineering Science 61 (2006), pp. 1741-1747. https://doi.org/10.1016/j.ces.2005.10.012, 2005.

Ludlam, F. H.: The heat economy of a rimed cylinder. In Q.J Royal Met. Soc. 77 (334), pp. 663–666. https://doi.org/10.1002/qj.49707733410, 1951.

Macklin, W. C.: The density and structure of ice formed by accretion. In Q.J Royal Met. Soc. 88 (375), pp. 30–50. https://doi.org/10.1002/qj.49708837504, 1962.

McDonell, V. G.; Samuelsen, G. S.: Sensitivity Assessment of a Phase-Doppler Interferometer to User-Controlled Settings. In E. D. Hirleman, W. D. Bachalo, P. G. Felton (Eds.): Liquid Particle Size Measurement Techniques: 2nd Volume. 100 Barr Harbor Drive, PO Box C700, West Conshohocken, PA 19428-2959: ASTM International, pp. 170-170-20, 1990.

McDonell, V. G.; Samuelsen, G. S.: Intra- and Interlaboratory Experiments to Assess Performance of Phase Doppler Interferometry. In Kenneth K. Kuo (Ed.): Recent Advances in Spray Combustion: Spray Atomization and Drop Burning Phenomena. Washington DC: American Institute of Aeronautics and Astronautics. 1996.

McDonell, V. G.; Samuelsen, G. S.; Wang, M. R.; Hong, C. H.; Lai, W. H.: Interlaboratory comparison of phase Doppler measurements in a research simplex atomizer spray. In Journal of Propulsion and Power 10 (3), pp. 402–409. https://doi.org/10.2514/3.23749, 1994.

McFarquhar, G. M.; Um, J.; Freer, M.; Baumgardner, D.; Kok, G. L.; Mace, G.: Importance of small ice crystals to cirrus properties. Observations from the Tropical Warm Pool International Cloud Experiment (TWP-ICE). In Geophys. Res. Lett. 34 (13), pp. n/a-n/a. https://doi.org/10.1029/2007GL029865, 2007.

McFarquhar, GM, Baumgardner, D, Bansemer, A et al. (17 more authors) Processing of Ice Cloud In-Situ Data Collected by Bulk Water, Scattering, and Imaging Probes: Fundamentals, Uncertainties and Efforts towards Consistency. Meteorological Monographs, 58. 11.1-11.3. ISSN 0065-9401, 2017.

Ofner, B.: Phase Doppler Anemometry. In Mayinger, F.; Feldmann, O.: Optical measurements techniques and application. 2nd edition, Springer, 2001.

Oleskiw, M. M; De Gregario, F; Esposito, B.: The effect of altitude on icing tunnel airfoil icing simulation. 1996.

Olsen, W.; Takeuchi, D.; Adams, K.: Experimental comparison of icing cloud instruments. AIAA-83-0026. Aerospace Science Converence. Reno, 1983.

Poots, G.; Gent, R. W.; Dart, N. P.; Cansdale, J. T.: Aircraft icing. In Philosophical Transactions of the Royal Society of London. Series A: Mathematical, Physical and Engineering Sciences 358 (1776), pp. 2873–2911. https://doi.org/10.1098/rsta.2000.0689, 2000.

ASTM E799-03, Practice for Determining Data Criteria and Processing for Liquid Drop Size Analysis, 2015.

Rudoff, R. C.; Bachalo, E. J.; Bachalo, W. D.; Oldenburg, J. R.: Liquid water content measurements using the Phase Doppler Particle Analyzer in the NASA Lewis Icing Research Tunnel. 31st ed. AIAA. Reno, Aerospace Sciences Meeting & Exhibit, 1993.

Rydblom, S.; Thornberg, B.: Liquid Water Content and Droplet Sizing Shadowgraph Measuring System for Wind Turbine Icing Detection. In IEEE Sensors J. 16 (8), pp. 2714–2725. https://doi.org/10.1109/JSEN.2016.2518653, 2016.

Rydblom, S.; Thornberg, B.; Olsson, E.: Field Study of LWC and MVD Using the Droplet Imaging Instrument. In IEEE Trans. Instrum. Meas. 68 (2), pp. 614–622. https://doi.org/10.1109/TIM.2018.2843599, 2019.

Snyder, H. E.; Senser, D. W.; Lefebvre, A. H.; Coutinho, R. S.: Drop size measurements in electrostatic paint sprays. In IEEE Trans. on Ind. Applicat. 25 (4), pp. 720–727. https://doi.org/10.1109/28.31253, 1989.

SPEC inc. FFSSP and FCDP Data Processing Manual,10/27/2012, http://www.specinc.com/sites/default/files/software_and_manuals/FCDP_Post%20Processing%20Software%20Manual_rev2.6_20121027.pdf

SPEC inc. C1C3_V4 manual, referenced to SPEC open source Matlab routines FCDP_C1_C3_V10, as of 01/15/2018

Stallabrass, J.R.: An Appraisal of the Single Rotating Cylinder Method of Liquid Water Content Measurement. In National Research Council of Canada Low Temperature Laboratory, Report LTR-LT-92, 1978.

Strapp, J. W. and R.S. Schemenauer, 1982: Calibrations of Johnson-Williams Liquid Water Content Meters in a High-Speed Icing Tunnel. J. Appl. Meteor., 21, 98–108, https://doi.org/10.1175/1520-0450(1982)021<0098:COJWLW>2.0.CO;2

Taylor, J. W., Haslett, S. L., Bower, K., Flynn, M., Crawford, I., Dorsey, J., Choularton, T., Connolly, P. J., Hahn, V., Voigt, C., Sauer, D., Dupuy, R., Brito, J., Schwarzenboeck, A., Bourriane, T., Denjean, C., Rosenberg, P., Flamant, C., Lee, J. D., Vaughan, A. R., Hill, P. G., Brooks, B., Catoire, V., Knippertz, P., and Coe, H.: Aerosol influences on low-level clouds in the West African monsoon, Atmos. Chem. Phys., 19, 8503-8522, https://doi.org/10.5194/acp-19-8503-2019, 2019.

Thornberry, T., Rollins, A., Avery, M., Woods, S., Lawson, P., Bui, P., Gao, R.-S., Ice water content-extinction relationships and effective diameter for TTL cirrus derived from in situ measurements during ATTREX 2014, 2017: J. Geophys. Res. Atmos., https://doi.org/10.1002/2016JD025948.

Tropea, C.: Optical Particle Characterization in Flows. In Annu. Rev. Fluid Mech. 43 (1), pp. 399–426. https://doi.org/10.1146/annurev-fluid-122109-160721, 2011.

Tuck, C. R.; Butler Ellis, M.C.; Miller, P.C.H: Techniques for measurement of droplet size and velocity distributions in agricultural sprays. In Crop Protection 16 (7), pp. 619–628. https://doi.org/10.1016/S0261-2194(97)00053-7, 1997.

Voigt, C., U. Schumann, P. Jessberger, T. Jurkat, A. Petzold, J.-F- Gayet, M. Krämer, T. Thornberry, D. Fahey: Extinction and optical depth of contrails, Geophys. *Res.* Lett., 38, L11806, https://doi.org/10.1029/2011GL047189, 2011.

Voigt, C; Schumann, U; Minikin, A. et al.: The Airborne Experiment on Natural Cirrus and Contrail Cirrus with the High Altitude Long-Range Research Aircraft Halo. Bulletin on the American Meteorological Society, https://doi.org/10.1175/BAMS-D-15-00213.1, 2017.

Weigel, R., Spichtinger, P., Mahnke, C., Klingebiel, M., Afchine, A., Petzold, A., Krämer, M., Costa, A., Molleker, S., Reutter, P., Szakáll, M., Port, M., Grulich, L., Jurkat, T., Minikin, A., and Borrmann, S.: Thermodynamic correction of particle concentrations measured by underwing probes on fast-flying aircraft, Atmos. Meas. Tech., 9, 5135–5162, https://doi.org/10.5194/amt-9-5135-2016, 2016.

Wendisch, M.; Pöschl, U.; Meinrat O. A. et al., ACRIDICON-CHUVA Campaign Studying Tropical Deep Convective Clouds and Precipitation over Amazonia Using the New German Research Aircraft HALO, Bulletin on the American Meteorological Society, https://doi.org/10.1175/BAMS-D-14-00255.1, 2016.

Widmann, J. F.; Presser; C.; Leigh, S. D.: Improving phase Doppler volume flux measurements in low data rate applications. In Measurement Science and Technology 12 (8), p. 1180, 2001.

Woods, S., P. Lawson, E. Jensen, T. Thornberry, A. Rollins, P. Bui, L. Pfister, M. Avery, Microphysical Properties of Tropical Tropopause Layer Cirrus, 2018: J. Geophys. Res. Atmos., https://doi.org/10.1029/2017JD028068

Zhu, J. Y.; Rudoff, R. C.; Bachalo, E. J.; Bachalo, W. D.: Number Density and Mass Flux Measurements Using the Phase Doppler Particle Analyzer in Reacting and Non-Reacting Swirling Flows. 31st AIAA. Reno, 1993. https://arc.aiaa.org/doi/pdf/10.2514/6.1993-361

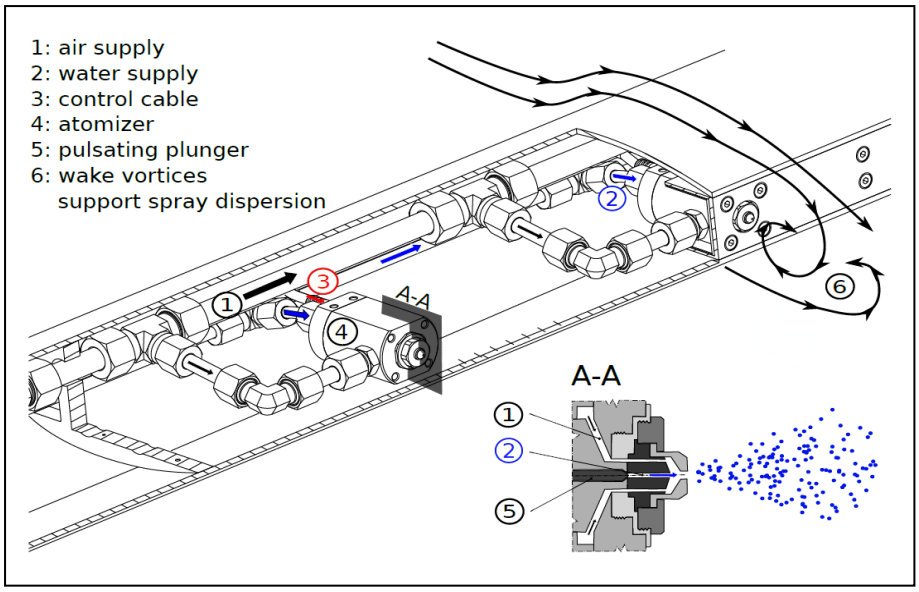

Figure 1: Spray system in the Braunschweig Icing Wind Tunnel (Bansmer et al. 2018).

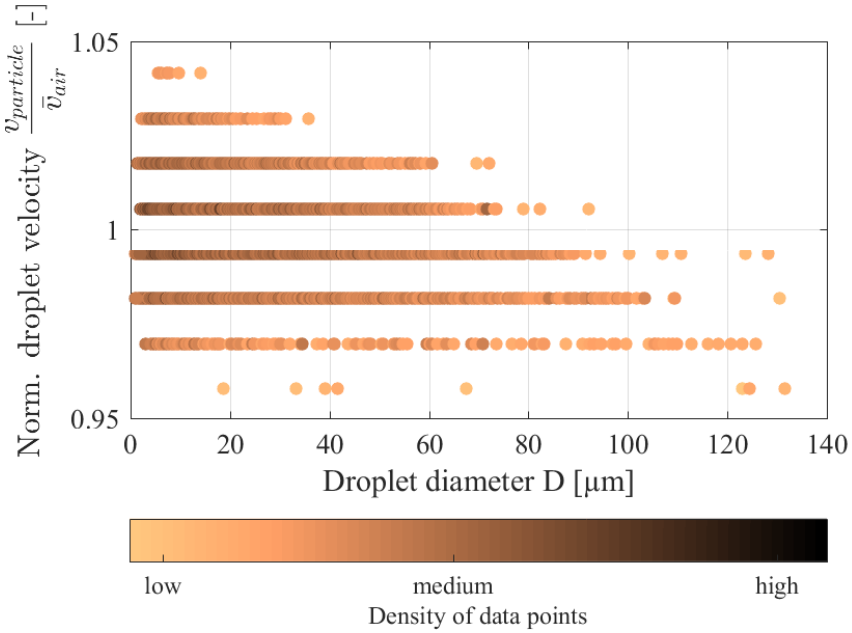

Figure 2: Droplet velocity over diameter (PDI Run 08/08/17 16:25).

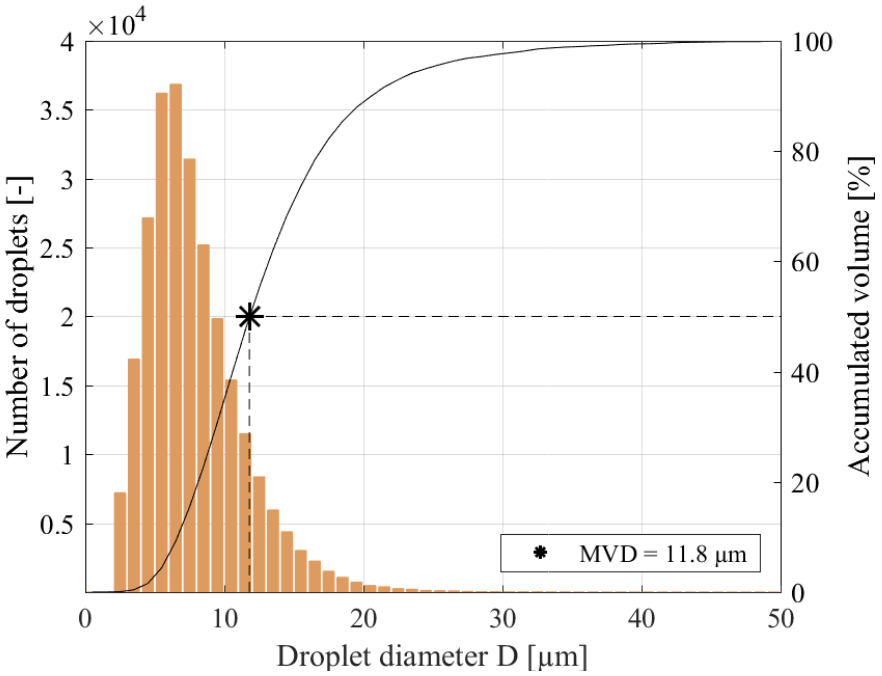

Figure 3: Droplet diameter histogram and cumulative volume curve at 20 m s^{-1} (PDI Run 18/04/19 17:19).

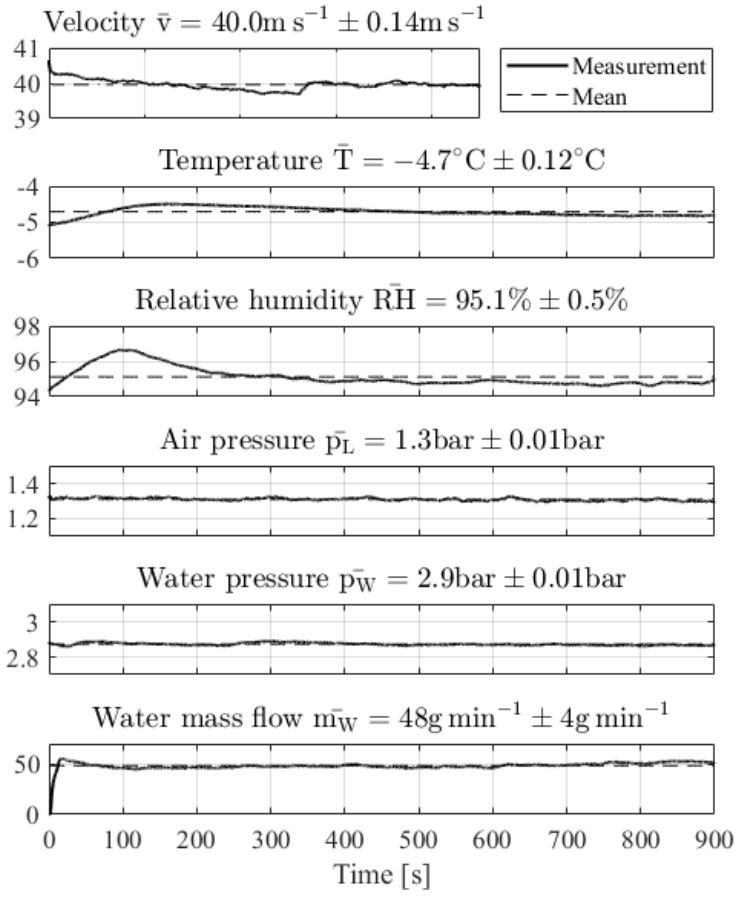

Figure 4: Exemplary stability of the wind tunnel conditions over 15 minutes test duration.

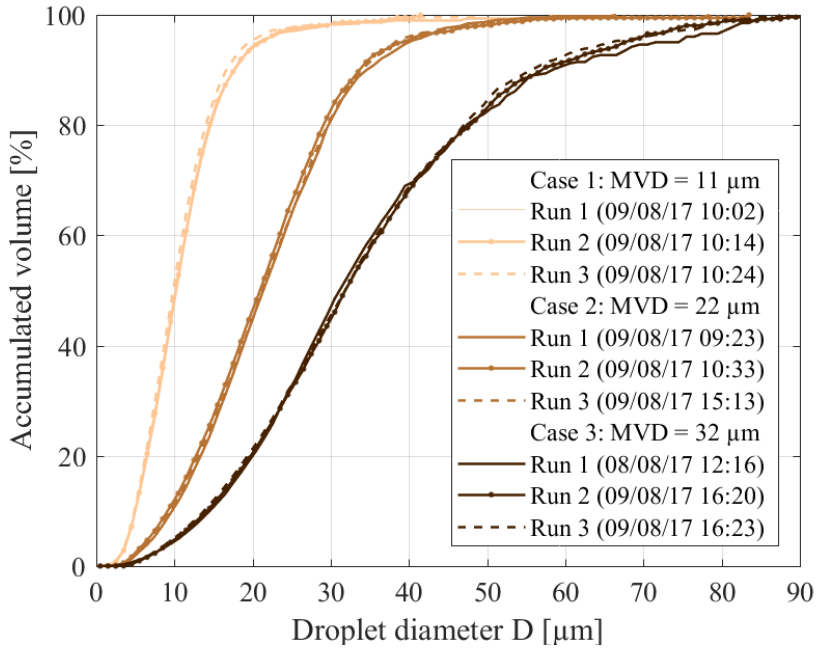

Figure 5: Wind tunnel repeatability shown with PDI measurements at 40 m s^{-1}, correlation coefficients R^2: Case 1: Run 1-2: R^2=1; Run 1-3: R^2=0,999; Run 2-3: R^2=0,999; Case 2: Run 1-2: R^2=0,926; Run 1-3: R^2=0,927; Run 2-3: R^2=1; Case 3: Run 1-2: R^2=0,999; Run 1-3: R^2=1; Run 2-3: R^2=1.

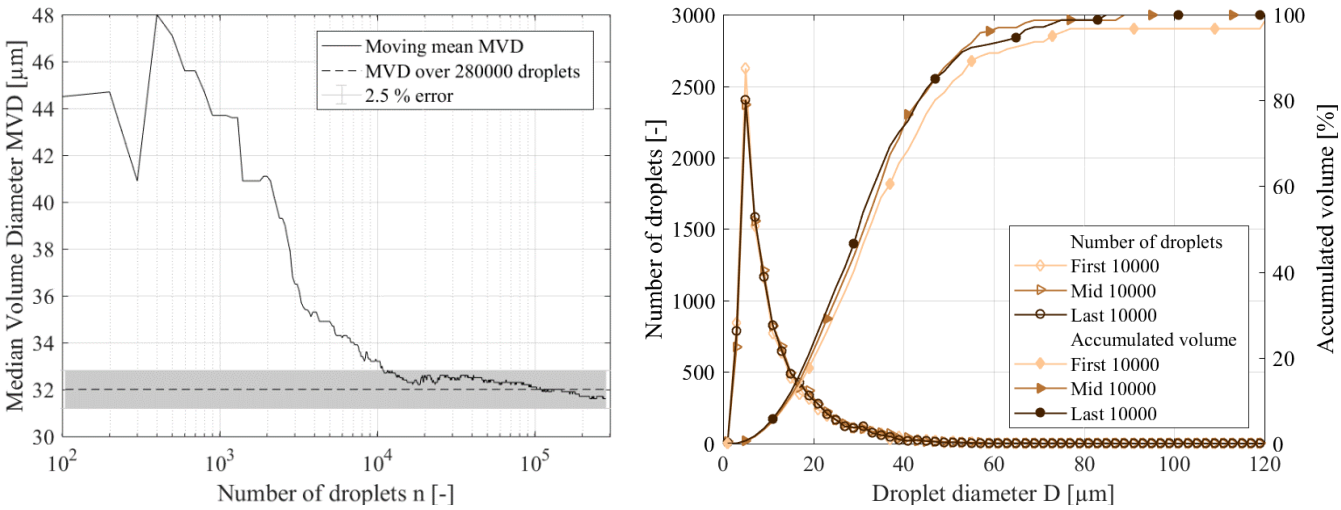

Figure 6: Convergence of MVD over number of droplets at 40 m s^{-1} and Temporal Stability (PDI Run 09/08/17 17:59).

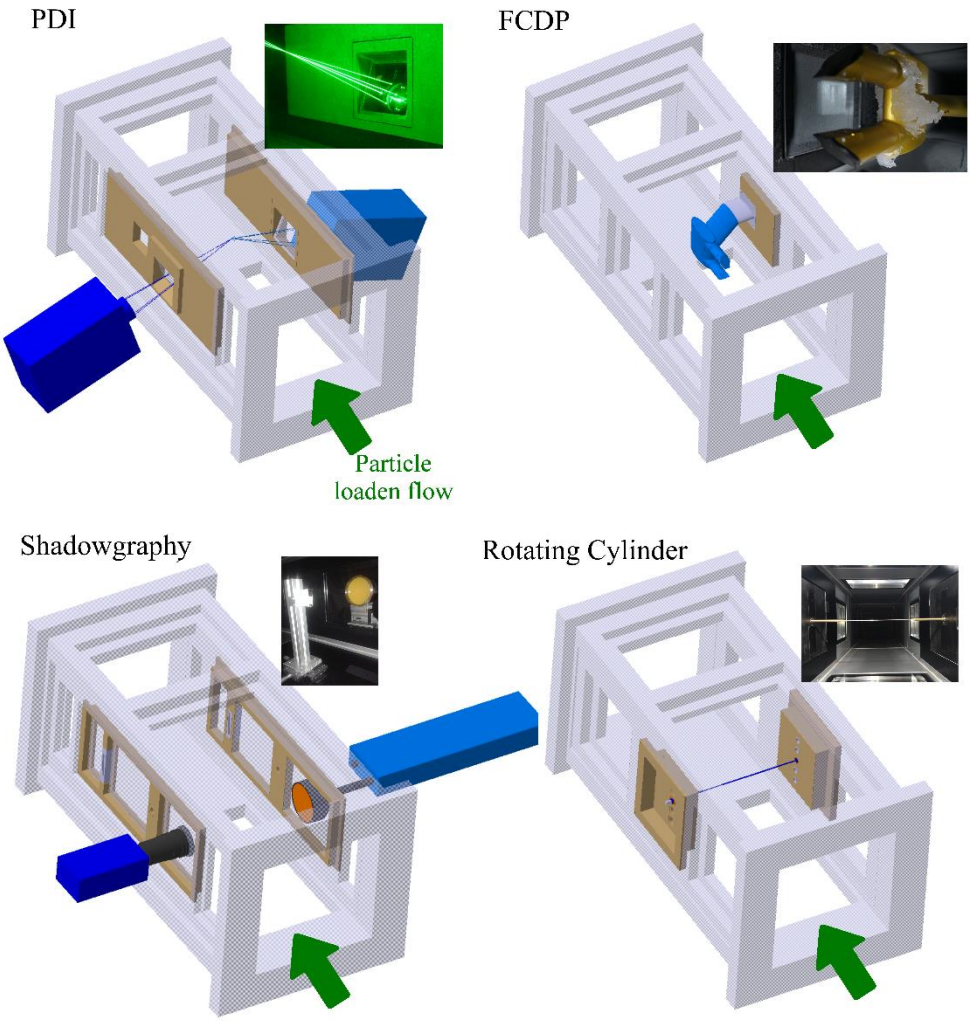

Figure 7: Measurement setups in the Braunschweig Icing Wind Tunnel.

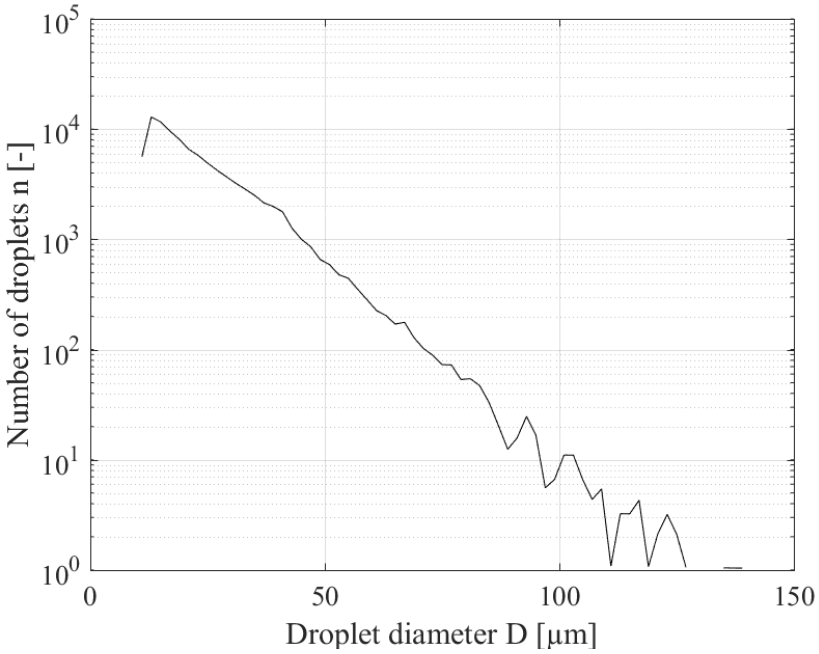

Figure 8: Number of droplets over diameter (PDI Run 18/04/19 18:25), total number of counts >95000.

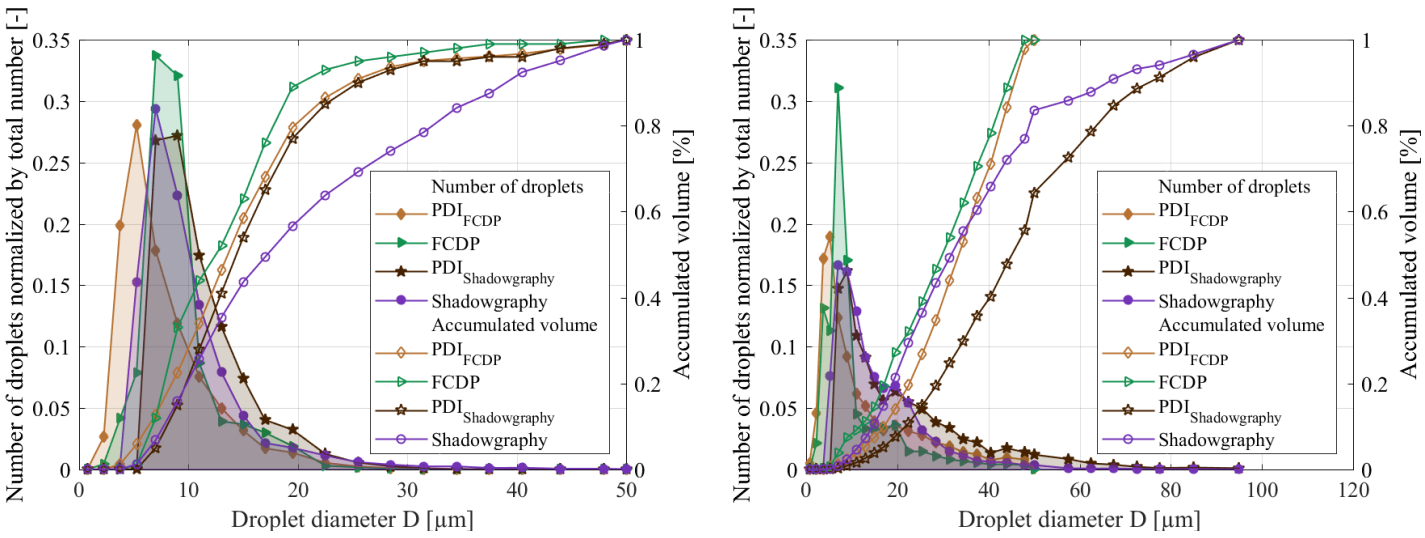

Figure 9: Droplet size distribution of different methods (left MVD 14.5µm, right MVD 33.8µm)

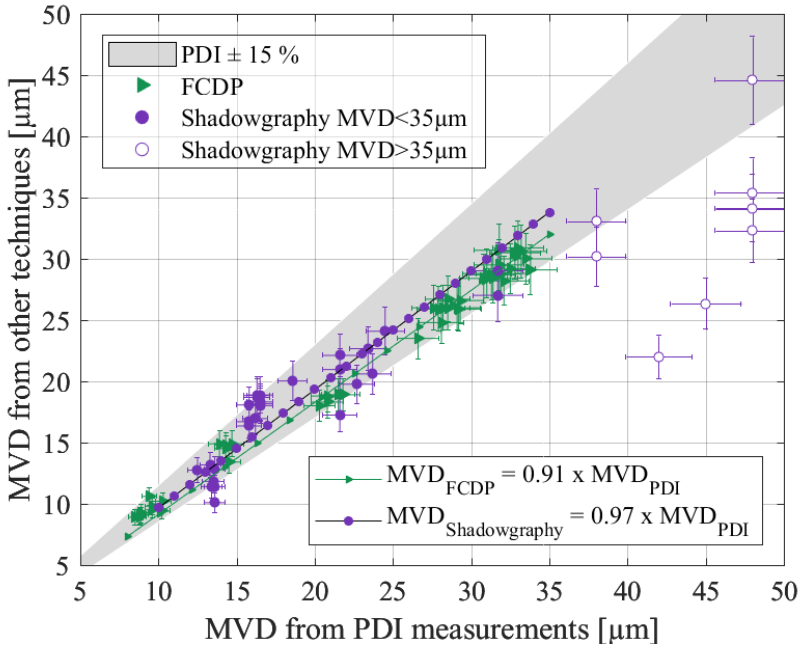

Figure10: Intercomparison of MVD measured with the PDI, the FCDP and the shadowgraphy.

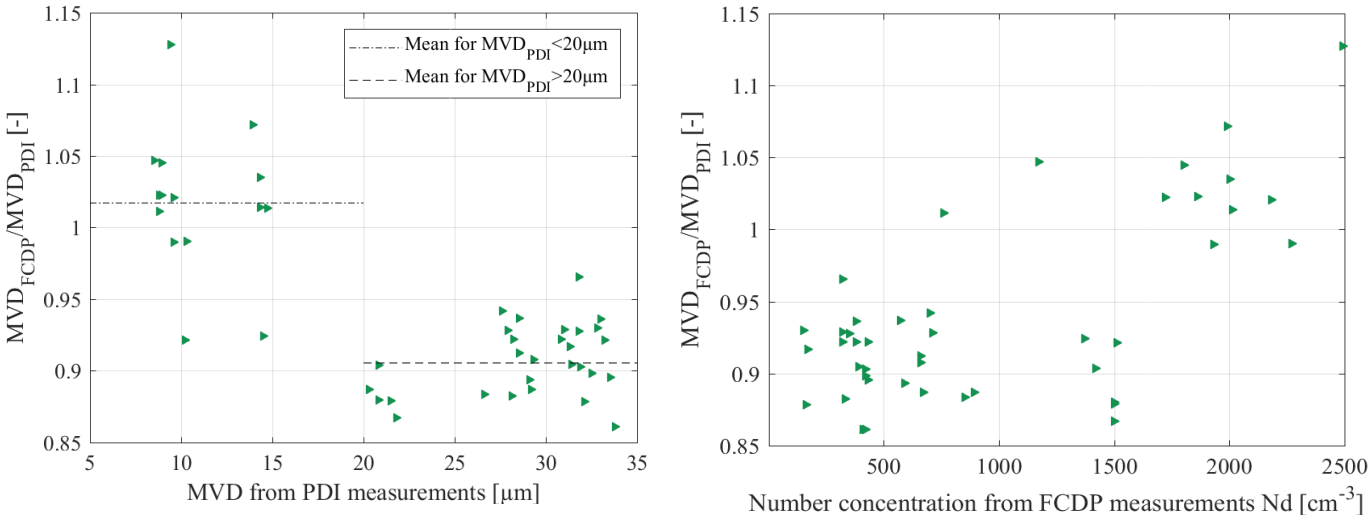

Figure 11: Effect of MVD on droplet size measurements from the FCDP (left) and effect of number concentration (right).

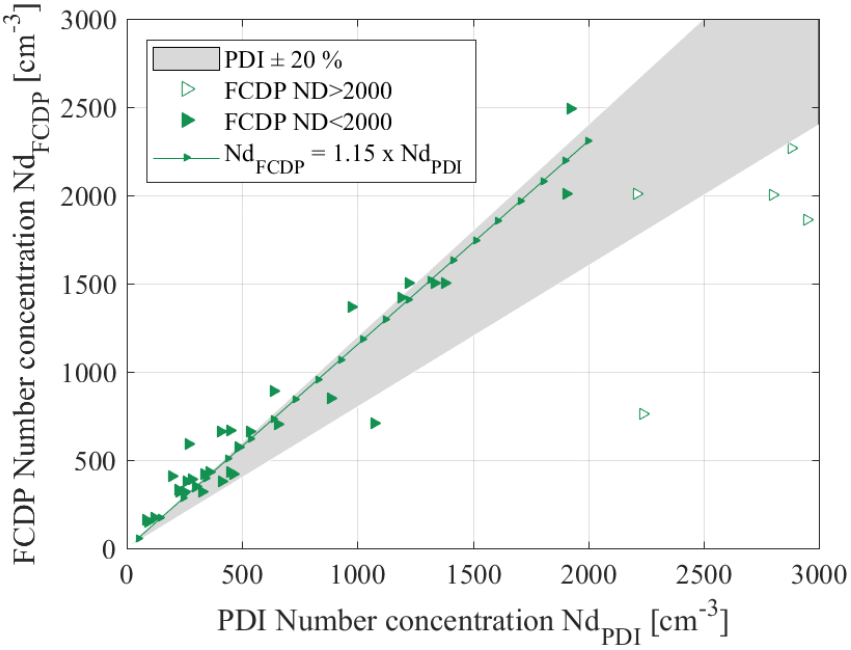

Figure 12: Comparison of Number Concentrations of PDI and FCDP.

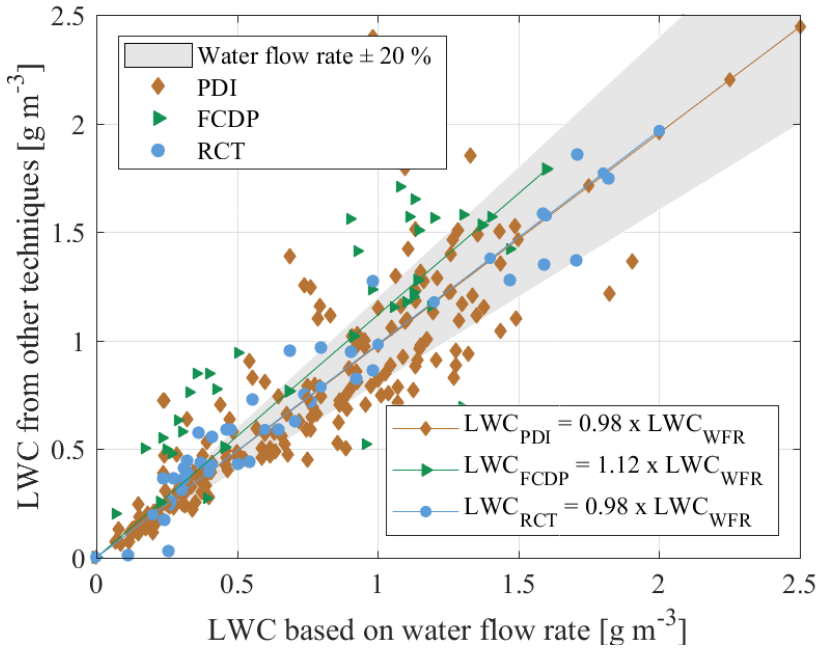

Figure 13: Intercomparison of LWC based on the water flow rate and measured with the PDI, the FCDP and the RCT.

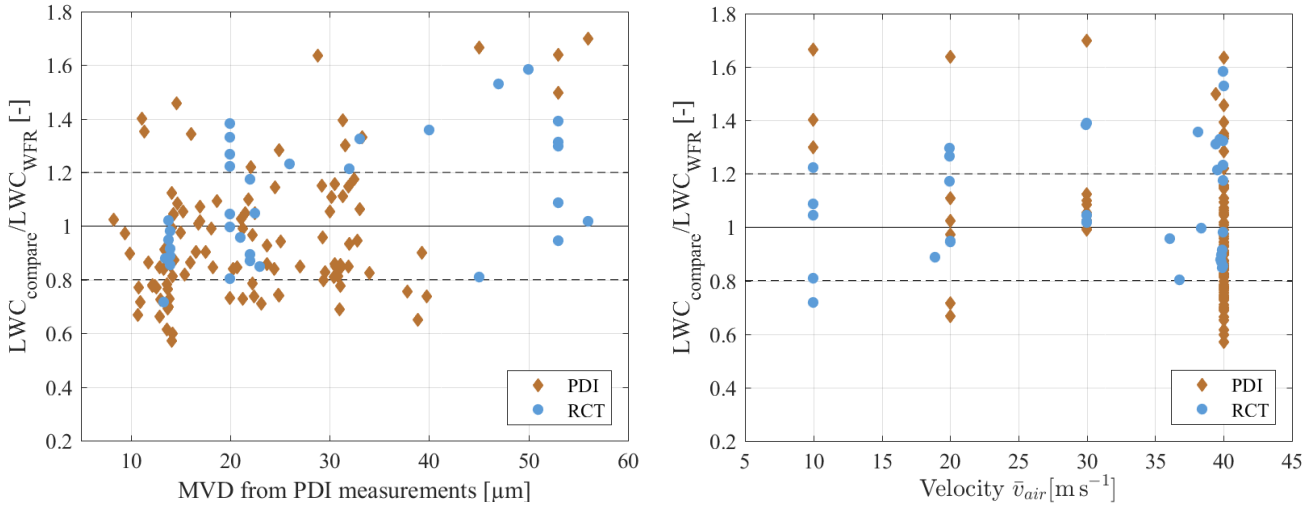

Figure 14: Effect of MVD (left) and effects of air velocity (right) on LWC measurements from the PDI and the RCT.

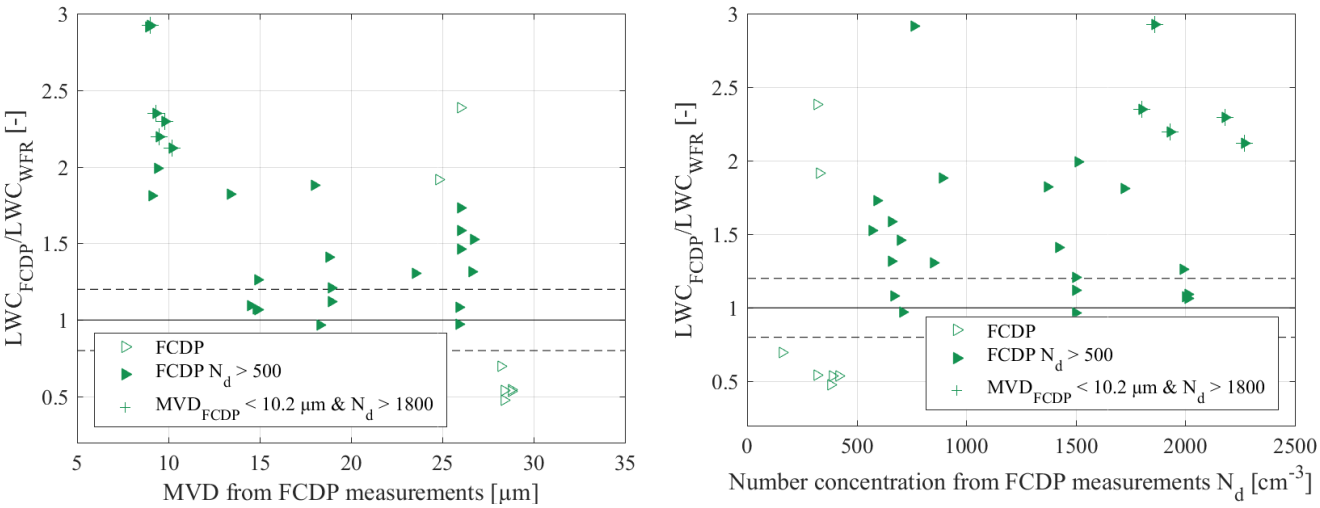

Figure15: Effect of MVD on LWC measurements from the FCDP (left) and effect of number concentration (right).

Table 1: Characteristic numbers of PDI setup Artium PDI-x00MD

Transmitter		**Receiver**	
Wave-length	532 nm	Focal length	500mm
Focal length	350 mm/ 500 mm	Collection Angle	40 ° ± 1°
Beam Separation	59.4 mm	Slit Aperture	100 µm
Beam diameter	2.33 mm	PMT Gain	300-500 V
Expander Factor	1	Domination scattering order	refraction
Frequency Shift	40 MHz		
Fringe Spacing	3.1 µm/ 4.5 µm	Static Range	0.9 - 134.4 µm 1.3 - 191.7 µm (2.6 -571.2 µm)
Beam Waist at probe volume	101.7 µm/ 145.4 µm		

Table 2: Characteristic numbers of FCDP (Serial No. 6) setup, SA and size calibration as of 4/28/2017

Wavelength	785 nm	DoF crit.	0.9
Domination scattering order	Forward Scattering	Bin number	21
Collection Angle	4-12 °	Bin widths	1.5-4 µm
Beam width diameter	0.08 cm	Size Range	1.5-50 µm
Qualifier Slit width	0.009 cm	Beam Waist	80 µm
DoF Rejection Crit.	0.9	Sample Area	0.09 mm²

Table 3: Characteristic numbers of shadowgraphy setup

Laser	Pulsed Nd-YAG laser	Camera	PCO Sensicam 12bit
Energy	1200 mJ	Resolution	1376 x 1070 px
Pulse duration	4 ns	Scale	1.9 x 1.9 µm ≙ 1 Pixel

Objective focus	180 mm, 1:1 macro	Tele convertor lens	1.4X
Aperture	3.5-32		

Table 4: Summarized instrument and test conditions

				PDI	FCDP	shadow-graphy	RCT
instrument measurement range	**velocity**	m s^{-1}	min	-130	10	x	1
			max	500	200	x	>175
	droplet diameter	µm	min	1	2	10	x
			max	134	50	200	x
	data rate / image rate	Hz	min	0	x	1	x
			max	>100000	x	2	x
	LWC	g cm^{-3}	min	x	0	x	0
			max	x	*2	x	1,9*3
tested range	**velocity**	m s^{-1}	min	10	30	10	10
			max	40	40	40	40
	MVD	µm	min	8,3	8,9	10,1	x
			max	56	30,9	44,6	x
	Coefficient of variation MVD*1	%		5	7	8	x
	LWC	g cm^{-3}	min	0,062	0,204	x	0,013
			max	2,434	1,707	x	1,858
	Coefficient of variation LWC*1	%		20	16	x	8
	number density	cm^{-3}	min	82	150	x	x
			max	3008	2270	x	x

*1 determined precision of measurement setup in BIWT, formula 2
*2 subject to coincidence
*3 Ludlam-limit at 40 m s^{-1}